NOAA Technical Memorandum ERL WPL-169

PROBABILITY DENSITY FUNCTION OF OPTICAL SCINTILLATIONS (SCINTILLATION DISTRIBUTION)

James H. Churnside
Richard J. Lataitis

Wave Propagation Laboratory
Boulder, Colorado
July 1989

noaa NATIONAL OCEANIC AND ATMOSPHERIC ADMINISTRATION / Environmental Research Laboratories

NOAA Technical Memorandum ERL WPL-169

PROBABILITY DENSITY FUNCTION OF OPTICAL SCINTILLATIONS (SCINTILLATION DISTRIBUTION)

James H. Churnside
Richard J. Lataitis

Wave Propagation Laboratory
Boulder, Colorado
July 1989

UNITED STATES
DEPARTMENT OF COMMERCE

Robert A. Mosbacher
Secretary

NATIONAL OCEANIC AND
ATMOSPHERIC ADMINISTRATION

Environmental Research
Laboratories

Joseph O. Fletcher
Director

NOTICE

Mention of a commercial company or product does not constitute an endorsement by NOAA Environmental Research Laboratories. Use for publicity or advertising purposes of information from this publication concerning proprietary products or the tests of such products is not authorized.

For sale by the National Technical Information Service, 5285 Port Royal Road
Springfield, VA 22161

CONTENTS

PROBABILITY DENSITY FUNCTION OF OPTICAL SCINTILLATIONS (SCINTILLATION DISTRIBUTION)

ABSTRACT

The probability density function of optical scintillation in the turbulent atmosphere is investigated theoretically and experimentally. The lognormally modulated Rician (LR) is the best available model for these fluctuations. For large apertures, this model reduces to a simple lognormal density function, which can be used under most practical situations.

1. INTRODUCTION

For modeling the performance of many electro-optical systems in the atmosphere, the probability density function (PDF) of optical irradiance is required. From the PDF, one can calculate the probability that some threshold level will be exceeded for laser radar detection probability calculations or receiver damage probability calculations. One can also calculate low-irradiance probabilities to obtain bit error rates for optical communications, miss probabilities for laser radar, or dropout rates for optical tracking systems. These examples are but a few of many possible system modeling applications.

It is generally accepted that the probability density function of optical scintillations will be lognormal, or very nearly so, after propagation through very weak turbulence in the atmosphere (Tatarskii, 1971). The theoretical argument for this distribution is based on the method of smooth perturbations (the Rytov approximation). In this approximation, the effect of turbulence is to perturb the propagating wave by a large number of independent, multiplicative events, and a central limit theorem argument leads to the lognormal distribution. The data seem to agree very well with this prediction.

Under conditions of extremely weak turbulence, conventional perturbation theory (the Born approximation) should be valid. Applying the central limit theorem to this expansion leads to a prediction that the optical amplitude should obey Rice-Nakagami statistics (Tatarskii, 1971) rather than lognormal. However, Strohbehn et al. (1975) showed that the Rice-Nakagami distribution approaches the lognormal as the variance becomes very small, which is the condition required by the Born approximation. This seems to resolve the conflict between the two expansions. In fact, Parry and Pusey (1979) have shown that all probability density functions have the same moments (and are therefore equivalent) in the limit of extremely small variances.

The probability density function after propagation through stronger turbulence or over greater distances is not as well understood. Some of the early measurements suggested that the fluctuations remained nearly lognormal even in very strong turbulence where the variance saturated (Gracheva and Gurvich, 1965; Gracheva, 1967; Fried et al., 1967; Ochs and Lawrence, 1969; Deitz and Wright, 1969). Wang and Strohbehn (1974)

showed theoretically that the irradiance fluctuations could not be purely lognormal in very high turbulence. In fact, it has been predicted that the density function of irradiance should approach a negative exponential in the limit of infinite turbulence (Dashen, 1979; DeWolf, 1968; Gochelashvili and Shishov, 1971; DeWolf, 1974). The argument is that the field at the observer is the sum of contributions from many independent scattering paths and should therefore have a circular Gaussian probability density function according to the central limit theorem. This implies a Rayleigh density function of the optical amplitude and a negative exponential density function of irradiance. However, if each contribution to the sum is a lognormal variate, the sum could remain very nearly lognormal under rather high turbulence levels, owing to the slow central limit theorem convergence of lognormal variates (Mitchell, 1968; Barakat, 1976; Consortini and Ronchi, 1977).

The extreme turbulence levels that produce Rayleigh amplitude statistics are not common, however, and under typical strong turbulence conditions, these statistics do not appear to be precisely lognormal (Wang and Strohbehn, 1974), Rayleigh (Gurvich et al., 1968), or Rice-Nakagami (Wang and Strohbehn, 1974). This realization has led to a number of proposed density functions that are combinations of these. DeWolf (1969) suggested a distribution that was Rice-Nakagami at low amplitudes and lognormal at very high amplitudes. Later, he proposed a density function based on a model of the optical field as a sum of a lognormal component and a Rayleigh component (DeWolf, 1974). Wang and Strohbehn (1974), and Strohbehn et al. (1975), suggested a density function based on the product of a Rice-Nakagami amplitude and a lognormal modulation factor.

The Rice-Nakagami and Rayleigh amplitude distributions are based on circular Gaussian statistics for the complex field amplitude. An attempt has been made to fit data better by replacing circular Gaussian statistics with the more general case of elliptical, or joint, Gaussian statistics; the real and imaginary components of the field are not assumed to be uncorrelated with equal variances. This distribution was introduced in the context of interplanetary radio star scintillation (Rino et al., 1976; Valley and Knepp, 1976) and later applied to the case of optical propagation through atmospheric turbulence (Knepp and Valley, 1978; Bissonnette and Wizinowich, 1979). In its most general form, this distribution has five adjustable parameters and is somewhat cumbersome. In very strong turbulence, the coherent component of the field is negligible, and the result is the Hoyt density function for the probability of normalized irradiance. Although this density function provides reasonable agreement with data, both experimental (Knepp and Valley, 1978) and theoretical (Bissonnette and Wizinowich, 1979) indications are that there is some multiplicative, lognormal process in the atmosphere that is not included in the elliptical Gaussian density function. Fremouw et al. (1980) considered a distribution consisting of an elliptical Gaussian field and a lognormal modulation factor. This was shown to provide a good description of radio propagation throughout the ionosphere. However, the addition of the lognormal modulation adds another parameter for a total of six.

In another approach to the problem, Furutsu (1972, 1976, 1979) and Ito and Furutsu (1982) applied the cluster approximation to the moment equation. For the special case of a Gaussian spectrum of turbulence, the moments can be found exactly and the characteristic function can be inverted to obtain the probability density function. Furutsu showed

that the logarithm of irradiance has a Rice-Nakagami density function in that case, which would occur if the effect of the atmosphere were to induce random tilts of the optical phase front. For the more realistic case of a Kolmogorov spectrum of turbulence, the moments of all orders cannot be found and neither therefore can the density function. A path integral approach to calculating the moments has been tried by Dashen (1984); it has similar limitations.

A much less rigorous approach than solving the moment equation was adopted by Parry et al. (1977). Physical intuition and the simplicity of the K distribution led them to compare the K distribution with the results of propagation experiments in strong turbulence (Parry and Pusey, 1979; Parry et al., 1977; Parry 1981) with very good results. The K distribution arises where one has a strong scattering process (random phase fluctuations of many wavelengths) with two distinct scale sizes (Jakeman and Pusey, 1976; Jakeman and Pusey, 1978; Newman, 1985). This fact makes the K distribution intuitively appealing for propagation through strong turbulence because of the observation of two distinct scale sizes in the received irradiance pattern under these conditions (Gracheva et al., 1978). Although it seems to fit the irradiance data better than either the lognormal or negative exponential distributions in strong turbulence, the K distribution has several problems. It can be applied only in cases of very high turbulence, and, even where it can be applied, it tends to underestimate the probability of high irradiances and thus underestimate higher order moments.

Phillips and Andrews (1981) made an extensive set of irradiance moment measurements and tried to improve on the K distribution on the basis of the data obtained. One such attempt (Phillips and Andrews, 1982) was to consider the field amplitude to be the sum of two components, each of which had an m distribution (closely related to the gamma distribution). The other (Andrews and Phillips, 1985) assumed a two-scale-size process like the K distribution, but used an n distribution to describe the smaller scale process. Neither of these density functions has gained the widespread acceptance of the K distribution.

Here, we reexamine the probability density function of irradiance introduced by Wang and Strohbehn (1975). The distribution results from the product of a Rice-Nakagami amplitude and a lognormal modulation factor. The required parameters can be calculated using the heuristic saturation theory of Clifford et al. (1974), Hill and Clifford (1981), and Hill (1982). This is a great advantage of this density function over a number of previous ones, which rely on parameters inferred from observed moments. With the understanding gained since this distribution was first proposed, we are in a position to answer the question raised by Knepp and Valley (1978): "Which physical processes give the lognormal and which the joint-Gaussian statistics?" We show that the heuristic theory suggests that the larger eddies in the turbulent medium produce the lognormal and the smaller ones the Gaussian statistics.

2. THE LOGNORMALLY MODULATED RICIAN PDF

Following Strohbehn et al. (1975), we write the observed field as

$$U = (U_C + U_G)\exp(\chi + iS) , \tag{1}$$

where U_C is a deterministic quantity, U_G is a circular Gaussian complex random variable, and χ and S are real Gaussian random variables. The irradiance is therefore given by

$$I = |U_C + U_G|^2 \exp(2\chi) , \tag{2}$$

where $|U_C + U_G|$ has a Rice-Nakagami probability density function and $\exp(2\chi)$ is lognormal.

The probability density function of irradiance can be calculated from

$$p(I) = \int_0^\infty p[I|\exp(2\chi)]\, p[\exp(2\chi)]\, d\ \exp(2\chi) , \tag{3}$$

where $p[a|b]$ represents the conditional density function of a given b. For the case at hand, we have the lognormally modulated Rician (LR) PDF

$$p(I) = \int_0^\infty dz \frac{(1+r)}{z} \exp\left(-r - \frac{1+r}{z} I\right) I_0\left[2\sqrt{\frac{(1+4)r}{z} I}\right]$$

$$\times \frac{1}{\sqrt{2\pi}\,\sigma_z z} \exp\left[\frac{\left(\ell nz + \frac{1}{2}\sigma_z^2\right)^2}{2\sigma_z^2}\right] , \tag{4}$$

where r is the coherence parameter $|U_C|^2 / < |U_G|^2 >$, z represents $\exp(2\chi)$, I_0 is the zero-order modified Bessel function of the first kind, and σ_z^2 is the variance of the logarithm of the irradiance modulation factor $\exp(2\chi)$. Unfortunately, an analytical evaluation of the integral of Eq. (4) has not been found.

For large irradiance, the integral of Eq. (4) can be approximated using the method of steepest descent. If we define the function

$$f(z) = \frac{(1+r)I}{z} - \ell n\left\{ I_0\left[2\sqrt{\frac{(1+r)r}{z}\, I} \right] \right\} + 2\ell nz$$

$$+ \frac{1}{2\sigma_z^2}\left(\ell nz + \frac{1}{2}\sigma_z^2 \right)^2 , \tag{5}$$

the density function can be approximated by

$$p(I) \approx \frac{1+r}{\sigma_z} |f''(z_0)|^{-1/2} \exp[-r - f(z_0)] , \tag{6}$$

where $f''(z_0)$ denotes the second partial derivative of f with respect to z and evaluated at z_0, where z_0 is the solution to the equation $f'(z_0) = 0$. However, this transcendental equation must be solved numerically, and it may be just as easy to perform the integration numerically.

Evaluation of the moments of the heuristic distribution is straightforward. Using Eq. (4) in the moment definition

$$< I^n >= \int_0^\infty dI\, I^n\, p(I) \tag{7}$$

yields an expression that can be evaluated analytically to get

$$< I^n >= \frac{(n!)^2}{(1+r)^n} \exp\left[\frac{1}{2} n(n-1)\sigma_z^2 \right] \sum_{m=0}^{n} \frac{r^m}{(n-m)!(m!)^2} . \tag{8}$$

3. PARAMETER VALUES

In order to calculate the LR PDF for any particular case, the two parameters of the PDF must be known. These can be calculated from the second and third moments of the normalized irradiance. They can also be approximated using a heuristic propagation theory.

3.1 Parameters from Moments

One obvious method of obtaining values for the parameters is from the second and third moments. The coherence parameter can be found by solving the polynomial equation

$$\frac{(r^2 + 4r + 2)^2}{(r + 1)^3(r^3 + 9r^2 + 18r + 6)} = \frac{< I^2 >^3}{< I^3 >} \tag{9}$$

for r. In Fig. 1, the moment ratio $< I^2 >^3 / < I^3 >$ is plotted as a function of the coherence parameter. Although it is a ratio of two sixth-order polynomials, the moment ratio is a single-valued function of r that varies from 4/3 for incoherent light to 1 for coherent light. Once r has been determined, the lognormal parameter σ_z^2 can be found from r and the second moment according to

$$\sigma_z^2 = \ell n \left[\frac{(r + 1)^2}{r^2 + 4r + 2} < I^2 > \right]. \tag{10}$$

In principle, one could start with the wave equation and a description of the medium and calculate the required second and third moments of irradiance. In practice such a calcula-

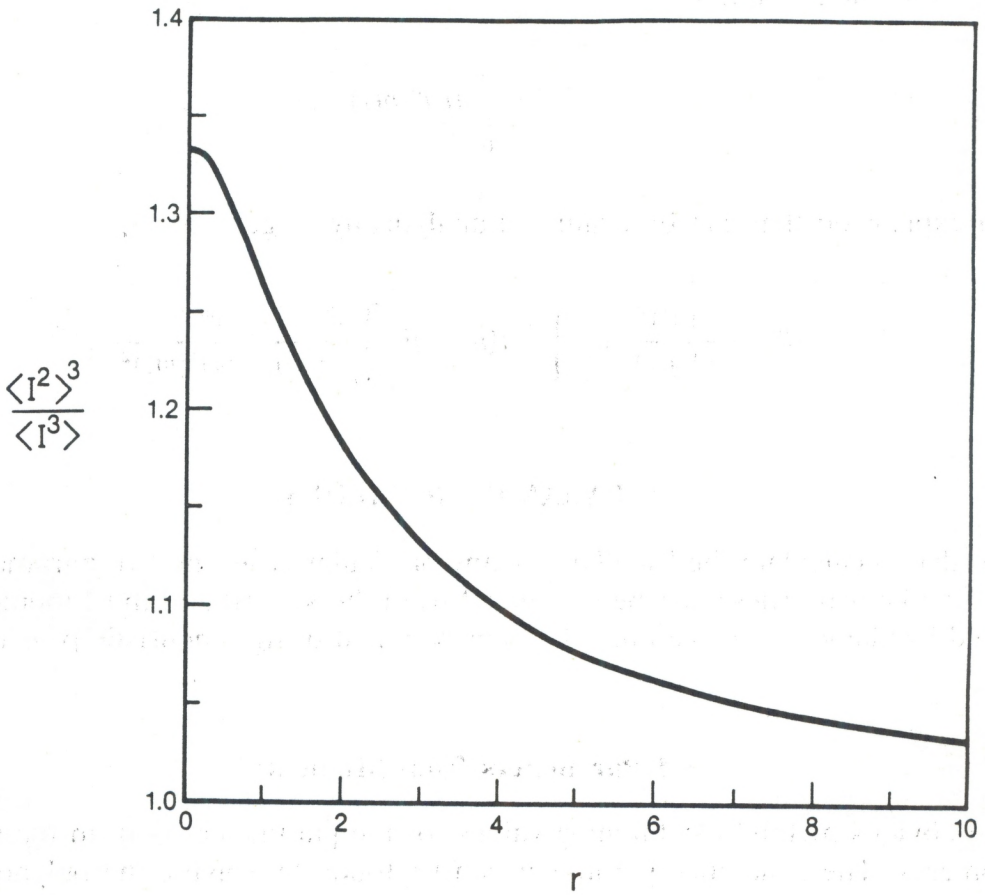

Figure 1. Moment ratio $< I^2 >^3 / < I^3 >$ as a function of coherence parameter r.

tion is extremely difficult, and it is probably more practical to use measured moments to estimate the parameters.

3.2 Parameters from Atmospheric Properties

Another method of obtaining parameter values is based on a physical model of turbulent scattering introduced by Clifford et al. (1974) and Yura (1974), and described in some detail by Strohbehn (1978). Simply, we recognize that the effect of a turbulent eddy that is larger than the Fresnel zone size at its position along the path can be described using geometrical optics. Each such eddy acts as a weak converging or diverging lens, and the total effect is the product of the effects from the individual eddies. Therefore, this is the process that produces the lognormal variations. The effectiveness of the eddies smaller than the Fresnel zone in focusing radiation is reduced because of diffraction. The smaller eddies also introduce a small-scale random phase distortion into the wave front, and thereby degrade the coherence of the wave. This is the process that produces the Rice-Nakagami variations. This reduction in coherence also reduces the focusing effectiveness of the larger eddies when the eddy size is larger than the coherence length ϱ_o. It is this process that leads to saturation of scintillation when the coherence length becomes less than the Fresnel zone size. From this physical picture, it seems clear that r should be the coherence of the wave over a Fresnel zone and σ_z^2 should be the geometric optics portion of the log-irradiance variance.

The lognormal parameter, σ_z^2, is that portion of the log-irradiance variance for which geometrical optics is valid. From the heuristic theory of saturation of optical scintillation, the total log-irradiance variance for spherical wave propagation can be written as (Hill and Clifford, 1981).

$$\sigma_{2\chi}^2 = 16\pi^2 k^2 L \int_0^1 du \int_0^\infty dK\, K\, \Phi_n(K) \sin^2\left[\frac{K^2 Lu(1-u)}{2k}\right] M_{ST}\left[\frac{KLU(1-u)}{k}\right], \qquad (11)$$

where k is the optical wavenumber, L is the propagation distance, u is the normalized position along the path, Φ_n is the spectrum of refractive index fluctuations in the atmosphere, K is the spatial wavenumber of those fluctuations, and M_{ST} is the short-term mutual coherence function. One commonly used spectrum is the Tatarskii model (Tatarskii, 1971) for the refractive index fluctuations:

$$\Phi_n(K) = 0.033 C_n^2 K^{-11/3} \exp(-0.0285 \ell_o^2 K^2)\,, \qquad (12)$$

where ℓ_o is the inner scale of turbulence and C_n^2 is the refractive turbulence structure parameter. This expression is valid within the inertial subrange. It does not apply for scale sizes larger than the outer scale. For scales near the inner scale and smaller, it is only an approximation. A more accurate model is available (Hill and Clifford, 1978), but only in

terms of a second-order differential equation that must be solved numerically. Within the inertial subrange or in the limit of zero inner scale, the two spectra both reduce to the Kolmogorov power-law spectrum.

The mutual coherence function, also from Hill and Clifford (1981), is given by

$$M_{ST}(\varrho) = \left\{ -48k^2 L \int_0^1 du' \frac{1}{u'^2} \int_0^\infty dK'\, K' \Phi_n\left(\frac{K'}{u'}\right) h(K') \left[1 - J_0(K'\varrho)\right] \right\} , \tag{13}$$

where J_o is the zero-order Bessel function of the first kind and h is a spectral cutoff function. It is given by

$$h(K') = K'\delta(K' - K) + H(K' - K) , \tag{14}$$

where δ is the Dirac delta function and H is the Heaviside step function. A similar expression exists for plane wave propagation (Hill, 1982); this case will not be considered explicitly.

We assume geometrical optics to be valid for turbulent eddies that are larger than the Fresnel zone. Therefore, we include contributions only from turbulent wavenumbers such that

$$K \leq \left[\frac{Lu(1-u)}{k}\right]^{-1/2} , \tag{15}$$

where the square root is the Fresnel zone size at path position u. Note that the validity of geometrical optics degrades smoothly with decreasing eddy size rather than abruptly as we have assumed here. With this approximation, the parameter σ_z^2 can be found from Eq. (11) by integrating K from 0 to the limit defined by Eq. (15) instead of from 0 to ∞. In the limit of zero inner scale, the calculation of σ_z^2 is greatly simplified. We have

$$\sigma_z^2 = 2.95\sigma_R^2 \int_0^1 du\, u^{5/6}(1-u)^{5/6} \int_0^{1/2} dy\, y^{1/6} \exp\left[-2.39\sigma_R^2\, y^{5/6} u^{5/6}\, (1-u)^{5/6}\right] , \tag{16}$$

where σ_R is the log-irradiance variance predicted for spherical wave propagation by the first-order Rytov theory, and is given by

$$\sigma_R^2 = 0.496k^{7/6}L^{11/8}C_n^2 \,. \tag{17}$$

The zero-inner-scale limit of σ_z^2 from Eq. (16) is plotted as a function of the Rytov variance in Fig. 2. For non-zero inner scales, the behavior of σ_z^2 is similar to that of the log-amplitude variance depicted in Fig. 7 of Hill and Clifford (1981). For very small inner scale values, the peak of the curve is lowered slightly and shifted to lower σ_R^2 values. As the inner scale increases, the peak value increases above the zero-inner-scale value. As the inner scale approaches the Fresnel zone size, the peak continues to increase and shifts to σ_R^2 values above that of the zero-inner-scale peak. For very large values of the inner scale, σ_z^2 can be approximated by

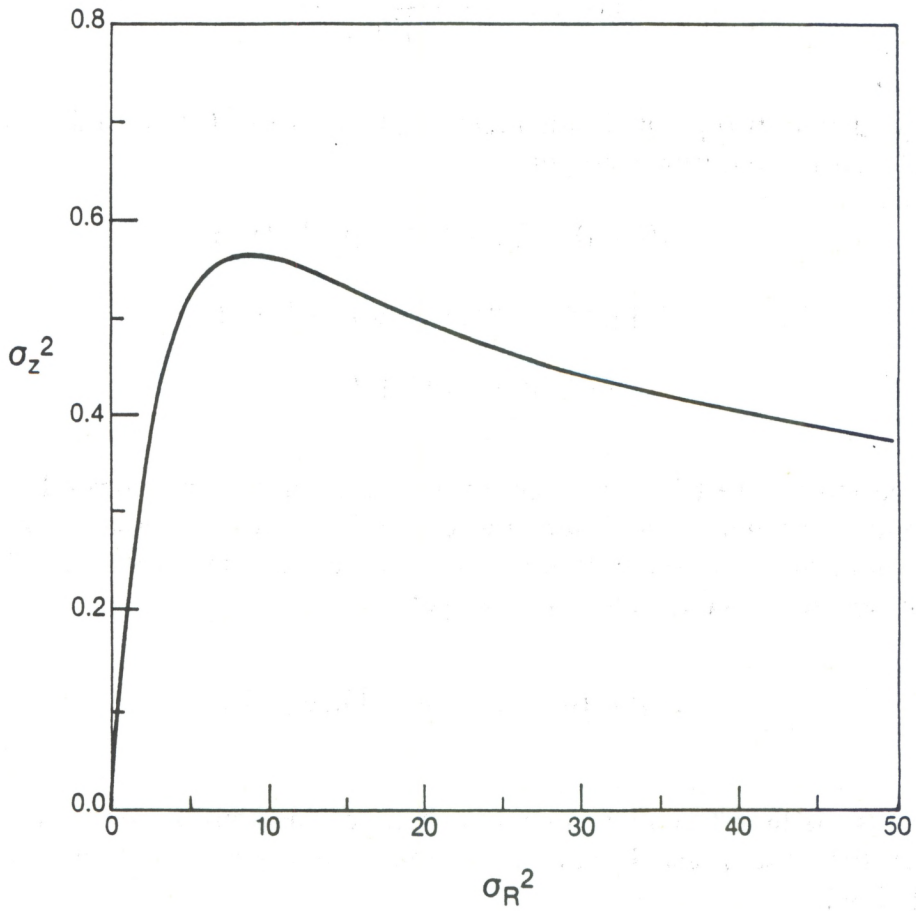

Figure 2. Log-modulation variance σ_z^2 as a function of Rytov log-irradiance variance σ_R^2 for zero inner scale.

$$\sigma_z^2 = 2.95\sigma_R^2 \int_0^1 du\, u^{5/6}(1-u)^{5/6} \int_0^{1/2} dy\, y^{1/6}$$

$$\times \exp\left[-1.32a^{1/3}\sigma_R^2 y\, u(1-u) - \frac{4y}{u(1-u)a^2}\right], \tag{18}$$

where

$$a = 8.37\sqrt{L/k\ell_o^2} \tag{19}$$

The coherence parameter, r, can be calculated from the mutual coherence function, which is defined as

$$M(\underline{x}_1, \underline{x}_2) = \frac{< U(\underline{x}_1)U^*(\underline{x}_2) >}{< |U|^2 >}\ , \tag{20}$$

where $\underline{x}_1$ and $\underline{x}_2$ denote two points in the receiver plane. If Eq. (1) is used to represent the field, Eq. (18) can be rearranged to get

$$< [U_C(\underline{x}_1) + U_G(\underline{x}_1)][U_C(\underline{x}_2) + U_G(\underline{x}_2)]^*$$

$$\times \exp[\chi(\underline{x}_1) + \chi(\underline{x}_2) + iS(\underline{x}_1) - iS(\underline{x}_2)] >$$

$$=< |U_C + U_G|^2 > \exp[2\chi] M(\underline{x}_1, \underline{x}_2)\ . \tag{21}$$

In this case, we wish to restrict our attention to the contributions from eddies for which geometrical optics are not valid. Under these conditions, the modulation parameters χ and S are constant over any separation of interest and disappear from Eq. (21). We can then let the separation become very large to get

$$|U_C|^2 = [|U_C|^2 +< |U_G|^2 >] M_{HF}(\infty)\ , \tag{22}$$

where $M_{HF}(\infty)$ is the high-frequency mutual coherence function, which is due to turbulent eddies smaller than the Fresnel zone, evaluated at infinite separation. The coherence parameter, defined as

$$r = \frac{|U_C|^2}{< |U_G|^2 >} \tag{23}$$

is given by

$$r = \left[\frac{1}{M_{HF}(\infty)} - 1\right]^{-1} . \tag{24}$$

The high-frequency mutual coherence function can be found from the short-term mutual coherence function by putting the Fresnel zone spatial frequency limit into the spectral cutoff function h to obtain

$$M_{HF}(\infty) = \exp\left\{-48k^2L \int_0^1 du \frac{1}{u^2} \int_0^\infty dK \Phi_n\left(\frac{K}{u}\right)\left[K\delta\left(K - \frac{1}{\sqrt{\frac{Lu(1-u)}{k}}}\right) + H\left(K - \frac{1}{\sqrt{\frac{Lu(1-u)}{k}}}\right)\right]\right\} . \tag{25}$$

For the case of zero inner scale, Eq. (25) can be integrated analytically. The resulting coherence parameter is given by

$$r = [\exp(0.398\sigma_R^2) - 1]^{-1} , \tag{26}$$

which is plotted in Fig. 3 as a function of the Rytov variance.

The normalized variance of irradiance can be calculated using these parameters and the formula

$$\sigma_I^2 = \frac{r^2 + 4r + 2}{(r+1)^2} \exp(\sigma_z^2) - 1 \tag{27}$$

obtained using Eq. (8). In Fig. 4, this is plotted as a function of the Rytov variance for the case of zero inner scale. The irradiance variance is nearly equal to the Rytov variance at very low values, reaches a peak value of about 2.5 at σ_R^2 of about 8, and decreases slowly to 1 at very large σ_R^2. This behavior is consistent with measured values. Parry and Pusey (1979) measured a peak intensity variance of about 4 at a σ_R^2 value somewhat larger than 4. Parry (1981) later measured a peak intensity variance of about 3.5 at σ_R^2 value of about 3. Phillips and Andrews (1981) measured peak values of about 3.5 at σ_R^2 values of 3–4 in one data set and of about 16 in another. Finally, Coles and Frehlich (1982) observed a peak of about 5 at a value of about 5. Despite quite a bit of scatter in all these data sets, each seems to define a curve similar to that in the figure. Some of the difference may be due to inner scale effects; in particular, a non-zero inner scale will produce a peak irradiance variance greater than 2.5.

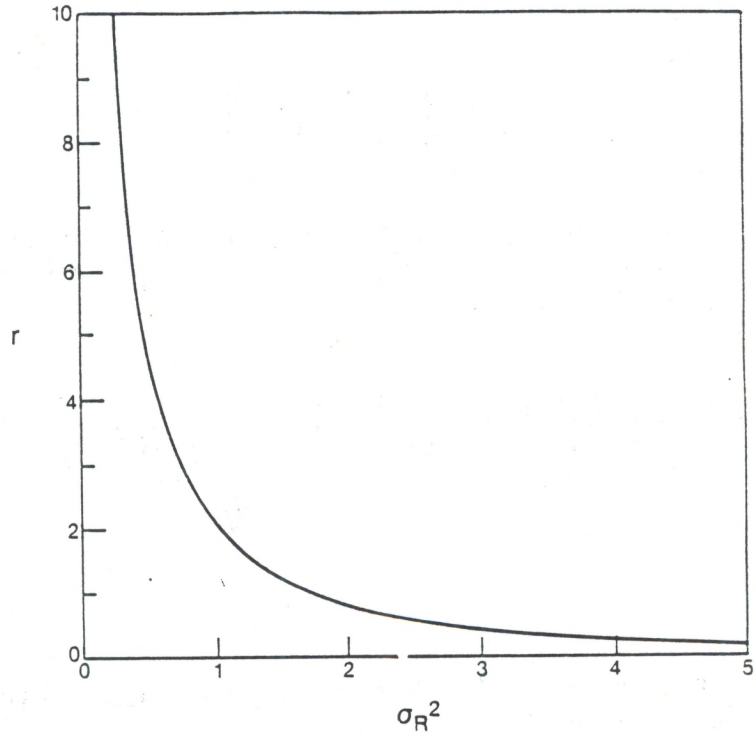

Figure 3. Coherence parameter r as a function of Rytov log-irradiance variance σ_R^2.

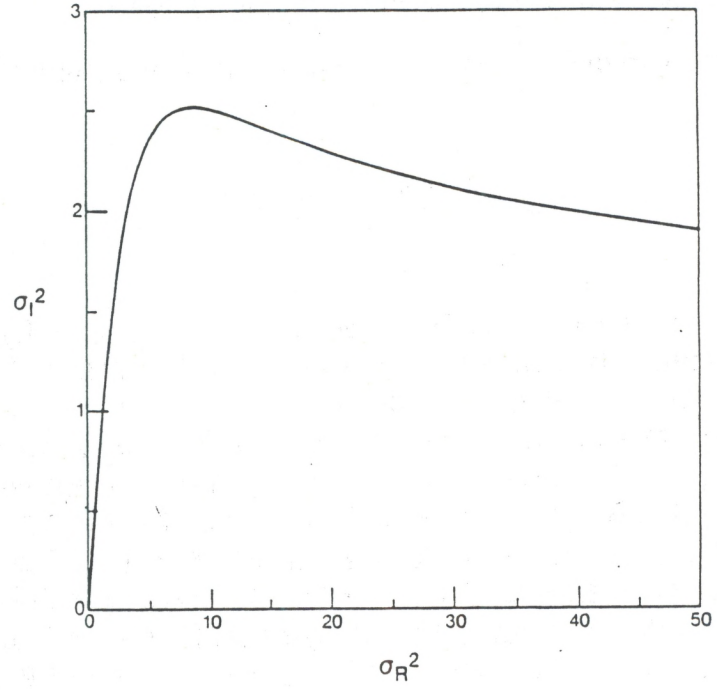

Figure 4. Normalized variance of irradiance σ_I^2 as a function of Rytov log-irradiance variance σ_R^2 for zero inner scale.

4. ASYMPTOTIC LIMITS

The general form of the LR PDF requires two parameters. However, in the limits of very weak and very strong path-integrated turbulence, the coherence parameter can be set to infinity or zero, respectively. In the former case, one has the lognormal PDF as previously mentioned. In the latter, one has a lognormally modulated negative exponential (LE) PDF.

4.1 Weak Turbulence Limit

In very weak turbulence, the parameters of the LR PDF are given by

$$\sigma_z^2 = 0.248\sigma_R^2 \tag{28}$$

$$r = 1/(0.398\sigma_R^2) \ . \tag{29}$$

The variance of irradiance can be approximated by

$$\sigma_I^2 = \sigma_z^2 + \frac{2}{r} = 1.04\sigma_R^2 \ , \tag{30}$$

which is very close to the accepted value of σ_R^2.

We expect that the distribution will be very nearly lognormal in this regime, with a log-intensity variance of σ_R^2. If we substitute Eqs. (26) and (27) into the moment equation (8) and expand to first order in σ_R^2, the result is

$$< I^n >= 1 + 0.522n(n-1)\sigma_R^2 \ , \tag{31}$$

which is very nearly the first-order expansion of the lognormal moments

$$< I^n >= \exp[0.500n(n-1)\sigma_R^2] \ . \tag{32}$$

Looking at the second and third moments, we see that r is infinite (hence a lognormal PDF) when $< I^2 >^3 =< I^3 >$. This can be seen from Eq. (9) and Fig. 1. Expanding Eq. (9) in a Taylor series in $1/r$ for large values of r yields

$$\frac{< I^2 >^3}{< I^3 >} = 1 + 6/r^2 \ . \tag{33}$$

Using Eq. (29), we can convert this to

$$\frac{\langle I^2 \rangle^3}{\langle I^3 \rangle} = 1 + 0.95\sigma_R^4 \,. \tag{34}$$

so the PDF will be very nearly lognormal when σ_R^4 is much less than 1.

Another technique that has been used to compare probability density functions with lognormal is to plot the integrated density function, or probability distribution function, on normal probability paper. A pure lognormal density function would plot as a straight line. This has been done for the LR density function in Fig. 5 for Rytov variances 1.0 and 0.1 and also for the limit as σ_R^2 approaches zero. We see that significant deviations from lognormal (recognized by significant curvature of the lines) do not appear until σ_R^2 begins to approach unity and these curves are in agreement with the data of Gurvich et al. (1968).

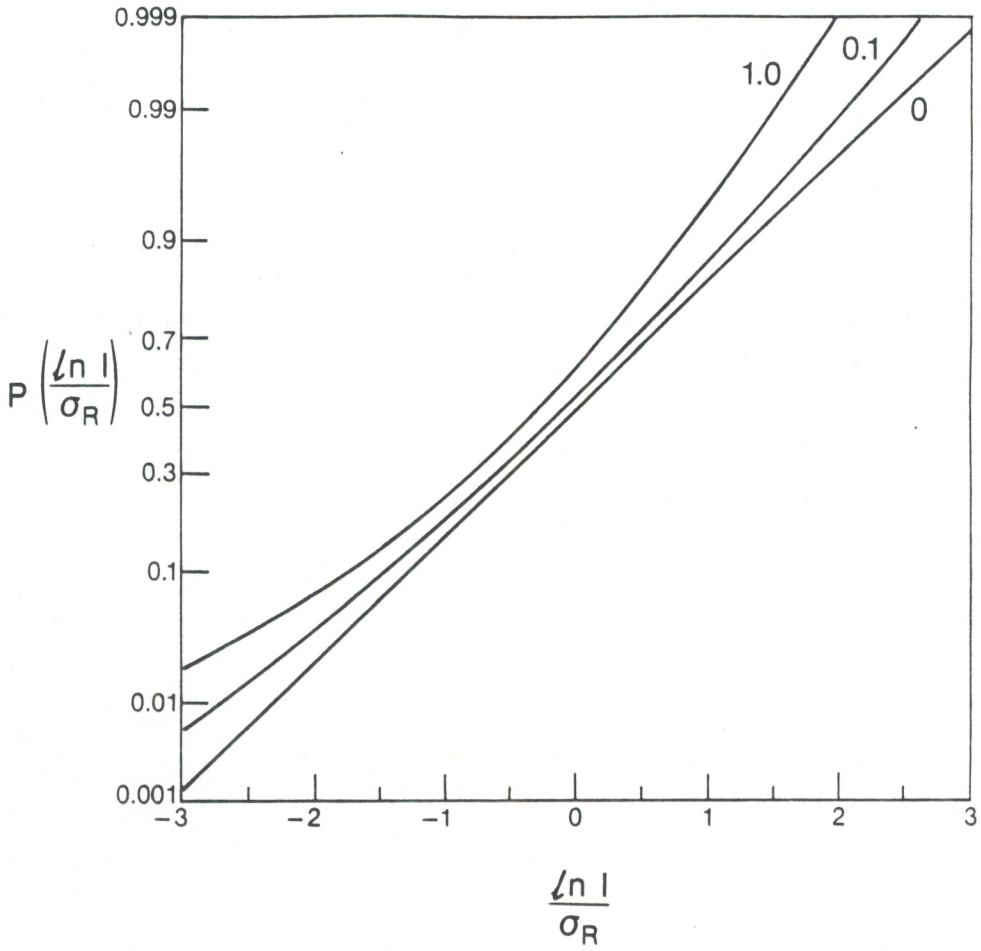

Figure 5. Probability distribution function of log-irradiance normalized by Rytov variance σ_R^2 for $\sigma_R^2 = 0$, 0.1, and 1.0. The vertical scale has been adjusted so that a lognormal distribution produces a straight line.

4.2 Strong Turbulence Limit

For the small-inner-scale case in very strong turbulence, we note that the exponential in Eq. (16) will be very small unless y is near zero. Therefore, little error is introduced if we extend the upper limit of the y integral to infinity. The integrals can then be evaluated with the result

$$\sigma_z^2 = 1.9\sigma_R^{-4/5} . \tag{35}$$

This expression overestimates σ_z^2 by about 34% at a Rytov variance of 10, but only by about 5% at 50. At very large inner scale values, a similar evaluation leads to

$$\sigma_z^2 = 4.1\alpha^{-7/18}\sigma_R^{-1/3} . \tag{36}$$

Of course, as the inner scale becomes very large, the amount of turbulence contributing to the scintillations becomes small. Equation (36) assumes large inner scale and also very strong scattering; conditions under which both of these assumptions are satisfied may be rare.

The coherence parameter is approximately given by

$$r = \exp(-0.398\sigma_R^2) , \tag{37}$$

which goes to zero very quickly. The Rice-Nakagami distribution in this case is very nearly Rayleigh, and the LR density function can be approximated by a lognormally modulated negative exponential function,

$$p(I) = \frac{1}{\sqrt{2\pi}\,\sigma_z}\int_0^\infty dz\,\frac{1}{z^2}\exp\left[-\frac{I}{z}-\frac{\left(\ell nz+\frac{1}{2}\sigma_z^2\right)^2}{2\sigma_z^2}\right], \tag{38}$$

which, although simpler than Eq. (4), still cannot be evaluated analytically. The moments can be found analytically, and are given by

$$< I^n >= n!\exp\left[\frac{1}{2}n(n-1)\sigma_z^2\right] . \tag{39}$$

Dashen (1984) showed that the intensity moments approach this form in strong turbulence, and this distribution is consistent with his result.

For zero inner scale, the normalized variance of intensity approaches

$$\sigma_I^2 = 1 + 3.8\sigma_R^{4/5} \tag{40}$$

at extremely large values of σ_R^2. For this same case, the asymptotic theory of Prokhorov et al. (1975) predicts a variance of

$$\sigma_I^2 = 1 + 1.9\sigma_R^{4/5} \tag{41}$$

These two theories predict the same σ_R dependence of intensity variance, and, since both these expressions are valid only when σ_R^2 is much greater than unity, the actual numerical values are fairly close. The discrepancy in the coefficients is disturbing, however, and deserves further study. For plane-wave propagation, the two theories are in much better agreement. The heuristic theory predicts the normalized intensity variance to be

$$\sigma_I^2 = 1 + 1.0\sigma_P^{4/5} , \tag{42}$$

where σ_P^2 is the Rytov variance for a plane wave and is given by 2.62 σ_R^2. The asymptotic theory predicts (Fante, 1983)

$$\sigma_I^2 = 1 + 0.86\sigma_P^{4/5} \tag{43}$$

and it appears that the heuristic theory more nearly describes plane wave propagation than spherical wave propagation through very strong turbulence.

5. THE IK PDF

The IK PDF of Andrews and Phillips (1985) is another two-parameter distribution that claims validity under all turbulence conditions. Therefore, data will also be compared with this distribution. The IK PDF has been described in detail elsewhere (Andrews and Phillips, 1985), but a brief review is presented here.

The IK PDF of the normalized irradiance I is given by (Andrews and Phillips, 1985)

$$\begin{aligned} p(I) &= 2\alpha(1+\varrho)\left[\frac{(1+\varrho)I}{\varrho}\right]^{(\alpha-1)/2} K_{\alpha-1}\left|2(\alpha\varrho)^{1/2}\right| \\ &\quad \times I_{\alpha-1}\{2|\alpha(1+\varrho)I|^{1/2}\} \quad \text{for} \quad I < \frac{\varrho}{1+\varrho} \\ &= 2\alpha(1+\varrho)\left[\frac{(1+\varrho)I}{\varrho}\right]^{(\alpha-1)/2} I_{\alpha-1}\left|2(\alpha\varrho)^{1/2}\right| \\ &\quad \times K_{\alpha-1}\{2|\alpha(1+\varrho)I|^{1/2}\} \quad \text{for} \quad I > \frac{\varrho}{1+\varrho} , \end{aligned} \tag{44}$$

where α is the effective number of scatterers, ϱ is the coherence parameter, and $K_{\alpha-1}$ and $I_{\alpha-1}$ are the modified Bessel functions. It has moments given by

$$< I^n >= \frac{n!}{\alpha^n (1+\varrho)^n} \sum_{k=0}^{n} \frac{\Gamma(\alpha+n)}{\Gamma(\alpha+k)} \frac{\alpha^k \varrho^k}{k!} , \tag{45}$$

where Γ is the gamma function.

The second and third moments are explicitly given by

$$< I^2 >= \frac{\varrho^2}{(1+\varrho)^2} + 2\frac{1+\alpha^{-1}}{1+\varrho}$$

$$< I^3 >= \frac{\varrho^3}{(1+\varrho)^3} + 3\frac{(1+2\alpha^{-1})\varrho^2}{(1+\varrho)^3} + 6\frac{(1+\alpha^{-1})(1+2\alpha^{-1})}{(1+\varrho)^2} . \tag{47}$$

Thus, the parameters ϱ and α can be estimated from the second and third moments by first solving the cubic equation

$$\begin{aligned}&(< I^2 >^2 - < I^2 > - \frac{1}{3} < I^3 > + \frac{1}{3})\varrho^3 \\ &+ (3 < I^2 >^2 - 2 < I^2 > - < I^3 >)(\varrho^2 + \varrho) + < I^2 >^2 - < I^2 > - \frac{1}{3} < I^3 >= 0\end{aligned} \tag{48}$$

for ϱ and using that value in

$$\alpha^{-1} = \frac{1}{2}(1+\varrho) < I^2 > - \frac{1}{2}\frac{\varrho^2}{1+\varrho} - 1 \tag{49}$$

to obtain α.

In very weak path-integrated turbulence, the coherence ϱ goes to infinity and the effective number of scatterers α goes to zero. The product of these two parameters is large. The moments for this case are given by

$$< I^n >= 1 + n(n-1)(\alpha\varrho)^{-1} . \tag{50}$$

Since the moments of any density function are given by

$$< I^n >= 1 + \frac{1}{2} n(n-1)\sigma^2 \tag{51}$$

when the variance σ^2 is small, we see that the variance of the IK PDF is $2/(\alpha\varrho)$ in weak turbulence. The PDF in this case has the form

$$p(I) = \frac{1}{\sqrt{2}\,\sigma} I^{-3/4} \exp\left(-\frac{2^{3/2}}{\sigma}|1-\sqrt{I}|\right). \tag{52}$$

In very strong path-integrated turbulence, the coherence parameter ϱ goes to zero and the IK PDF reduces to the K PDF (Parry and Pusey, 1979),

$$p(I) = \frac{2}{\Gamma(\alpha)} \alpha^{(\alpha+1)/2} I^{(\alpha-1)/2} K_{\alpha-1}[2(\alpha I)^{1/2}], \tag{53}$$

which has moments

$$< I^n >= \frac{n!}{\alpha^n} \frac{\Gamma(\alpha+n)}{\Gamma(\alpha)}. \tag{54}$$

The parameter α is found from

$$\alpha^{-1} = \frac{1}{2} < I^2 > - 1. \tag{55}$$

6. EXPERIMENTS

Two series of experiments were conducted to investigate the validity of the LR PDF. To obtain low to moderate path-integrated turbulence values, data were collected on several days during the summer and fall of 1987. At different times, path lengths of 50, 100, 400, 1200, and 2400 m were used. All paths were horizontal and were at heights of 1.5 m to 2 m above flat, uniform grassland. Optical instruments for measuring path-averaged values of cross-wind, turbulence strength C_n^2, and inner scale ℓ_o were operating over paths near and parallel to each of the propagation paths during the experiments.

The measurement configuration is depicted in Fig. 6. Light from the laser is diverged and allowed to propagate through the turbulent atmosphere. For the shorter paths (<1 km), the source was a 5-mW He-Ne laser whose divergence was adjusted depending on the path length. The source for the longer paths was an Ar^+ ion laser producing 300 to 500 mW of 488-nm radiation. It was diverged to 4 mrad. After propagation through turbulence, the optical signal was passed through an interference filter to remove background light, passed through an aperture, and detected. For the He-Ne signal, the aperture was the 200-μm-square active area of the silicon photodiode. The Ar^+ ion signal

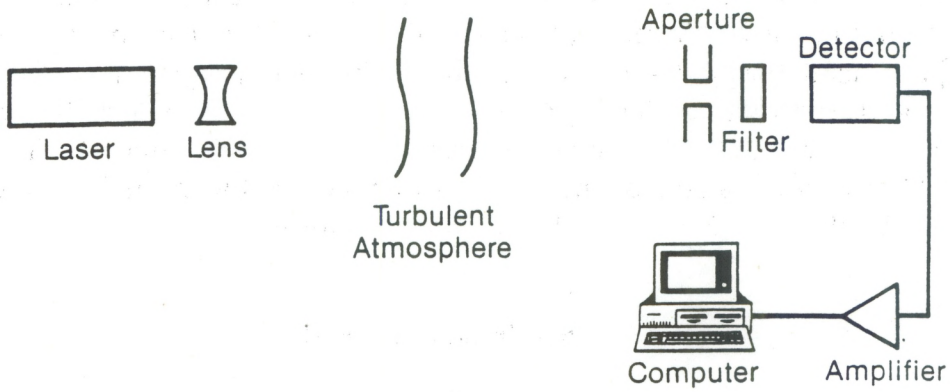

Figure 6. Apparatus used for PDF measurements.

was detected by a photomultiplier tube behind a 250-μm-diameter circular aperture. In both cases, the detected signal was amplified with a 10-kHz bandwidth and fed into a microcomputer, where it was sampled, digitized, and recorded for later processing.

Each data run consisted of a number of repetitions of a collection cycle lasting just over 1 minute. For the shorter paths, the cycle consisted of 32,000 data samples at 500 samples/second, followed by 6400 samples taken while the laser was blocked. This was accomplished automatically by the computer using a radio link to the laser shutter. The cycle was completed by recording cross-wind, turbulence strength, and inner scale values. Each data run consisted of 29 such cycles. For the longer paths, the process was the same, except that 64,000 samples were recorded at 1000 samples/second in each cycle and 70 cycles went into each data run.

Data processing involved computation of the second and third moments and of histograms of probability. In each case, the data were corrected for any offsets and normalized by the average signal level. Generally, each data run was processed as a unit. The exceptions to this were long-path data taken near dawn and dusk when turbulence was low but rapidly changing. In these cases, each cycle of data was processed separately. The noise variance of each data run or cycle was calculated and found to be negligible except for the 400-m cases.

The configuration of Fig. 6 was also used to measure the probability density function of intensity during periods of high path-integrated turbulence in August 1985. A 40-mW He-Ne laser operating on the 633-nm line was used as the radiation source. The natural beam divergence is about a milliradian. Since changes in vertical temperature gradient along the path could conceivably move the beam up or down by some reasonable fraction of this width, a negative cylindrical lens was used to expand the vertical beamwidth by about a factor of 2. The propagation range was 1 km at a height of about 2 m above the surface, which was flat, uniform grassland. At the receiver, the signal was detected by a photomultiplier tube after passing through a 1-mm aperture and a 1-nm optical bandpass filter. After amplification, the intensity signal was fed into the computer.

In the computer, the intensity signal was digitized with 12 bits of resolution at a rate of 5000 samples per second. After 10,833 samples had been collected, the system sampled the output of an incoherent optical scintillometer. This instrument provides a measure of C_n^2 averaged over a 25-m path parallel to the main propagation path. After C_n^2 was sampled, the data record, including C_n^2 was stored on the system disk for later processing. Each data run consisted of 50 such records, or a little more than 1/2 million intensity samples. After each data run, a single record was recorded with the laser blocked to allow estimation of offsets and noise in the receiver electronics.

6.1 Irradiance PDF

A typical PDF for the 50-m path is plotted in Fig. 7. The measured variance for this case was 2.6×10^{-3}, so the path-integrated turbulence is very low. From the linear plot (a), we see that the data appear to be very nearly Gaussian. The calculated parameters of the LR PDR were $\varrho = \infty$ and $\sigma_z^2 = 2.6 \times 10^{-3}$, and the LR PDF was lognormal for this case. With such a small variance, the lognormal is also very nearly Gaussian. However, the calculated lognormal underestimates the peak of the data by about 5% and it seems the measured variance is slightly high. From the logarithmic plot 7(b), we see that the data begin to deviate from lognormal at irradiance values greater than about 3 standard deviations from the mean. This would tend to make the measured variance slightly higher than one would expect from a purely lognormal process. We hypothesize that these values are due to the intermittency of atmospheric turbulence; brief periods of very strong turbulence during the measurement time would produce a few irradiance values with relatively large deviations from the mean.

For the IK PDF, $\varrho = 157$ and $\alpha = 4.9$ and the PDF was very nearly given by the weak-turbulence limit of Eq. (52). We see that the IK PDF overestimates the peak probability by about 40%. It also has a cusp at the peak that is not representative of the data. Generally, the IK PDF is a very poor match to these data.

Figure 8 is a typical case for the 100-m path. In this example, the measured variance was 0.12. The LR PDF is still lognormal in this regime with a log-irradiance variance of 0.12. As before, the peak probability is underestimated by a few percent (4%) and the probability on the tail is overestimated, but the general shape of the data is very nearly lognormal within about 5 standard deviations of the mean. The parameters for the IK PDF were $\varrho = 23$ and $\alpha = 0.69$. Again, the IK PDF significantly overestimates the peak probability and comes to a very sharp peak that is not representative of the data.

Figure 9 presents data taken on the 2400-m path during the low turbulence conditions. The measured variance was 1.3. In this case, the LR PDF is beginning to deviate from lognormal. The coherence parameter $\varrho = 1.7$ and $\sigma_z^2 = 0.36$, which leads to a very good fit to the data. Note that these data were taken over a much shorter time period, and the effects of intermittency are not as noticeable. For the IK PDF, $\varrho = 0.27$ and $\alpha = 2.3$. The IK is a sharply peaked function that does not fit the data at all near the peak. We

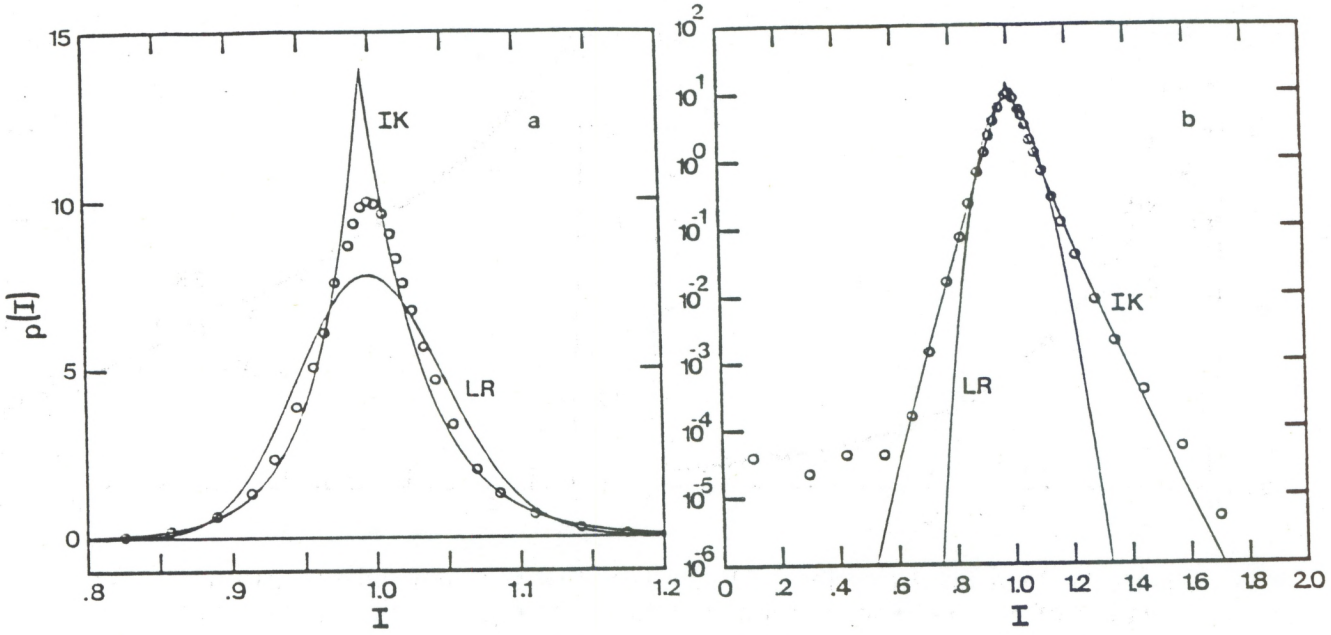

Figure 7. Measured (circles), LR, and IK PDFs of normalized irradiance for variance of 2.6×10^{-3}. (a) Linear representation; (b) logarithmic representation.

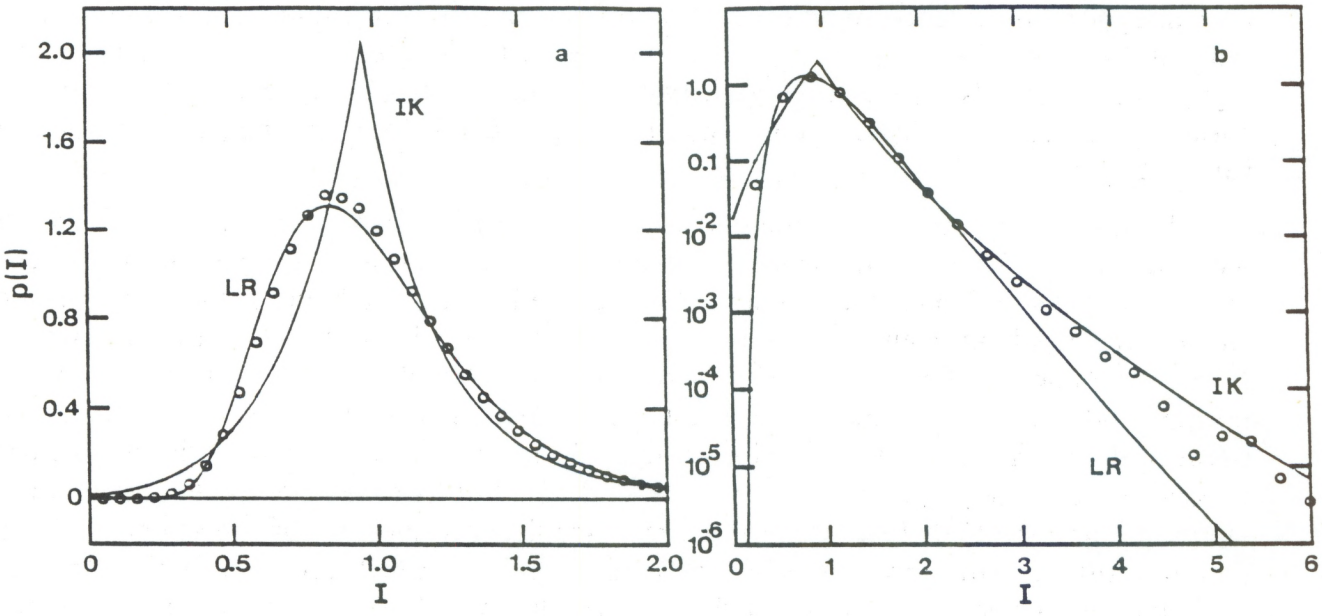

Figure 8. Measured (circles), LR, and IK PDFs of normalized irradiance for variance of 0.12. (a) Linear representation; (b) logarithmic representation.

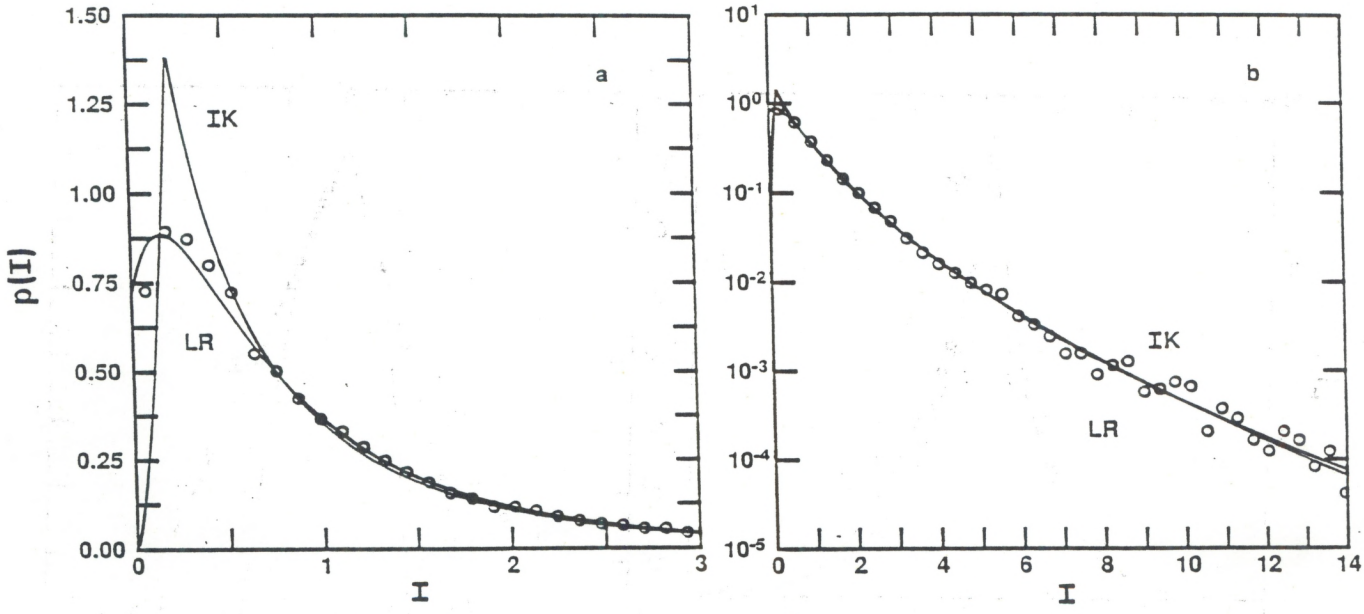

Figure 9. Measured (circles), LR, and IK PDFs of normalized irradiance for variance of 1.3. (a) Linear representation; (b) logarithmic representation.

should point out that another possible solution exists for the IK PDF: $\varrho = 21.7$ and $\alpha = 0.068$. However, this leads to a PDF with a peak at $I = 0$ and a second peak at $I \approx 1$ that is a worse representation of the data than the solution that was chosen. Care must be taken to ensure that the most reasonable solution to the IK PDF is used. No such ambiguity exists with the LR PDF.

For the 1000-m data, σ_R^2 ranged from 12 to 43. These values are well into the strong path-integrated turbulence regime where $r = 0$ and the LR PDF reduces to the single-parameter LE PDF. Similarly, the IK PDF reduces to the single-parameter K PDF. In this regime data can also be compared with the lognormal PDF, which also has a single parameter. In each case, the required parameter was found from the measured irradiance variance.

Figure 10 represents the data run with the lowest irradiance variance out of the 10 data runs ($\sigma_I^2 = 2.83$). Comparing the theoretical density functions, one finds that the lognormal density function is higher than the K PDF for irradiance values from some small value to about 2 and for values greater than about 17. Elsewhere, the K is higher than the lognormal. The lognormally modulated exponential function is between the lognormal and the K functions at all irradiance values. The data points also tend to lie between the K and lognormal functions. Figure 11 represents the data run with the highest irradiance variance of the 10 data runs ($\sigma_I^2 = 4.13$). In this case, the points at which the lognormal and the K PDFs cross are at larger irradiance values, occurring at about $I = 2.5$ and 23. Although the three density functions are fairly close together over the range of available data values, the data favor the lognormally modulated exponential PDF over the lognormal or the K.

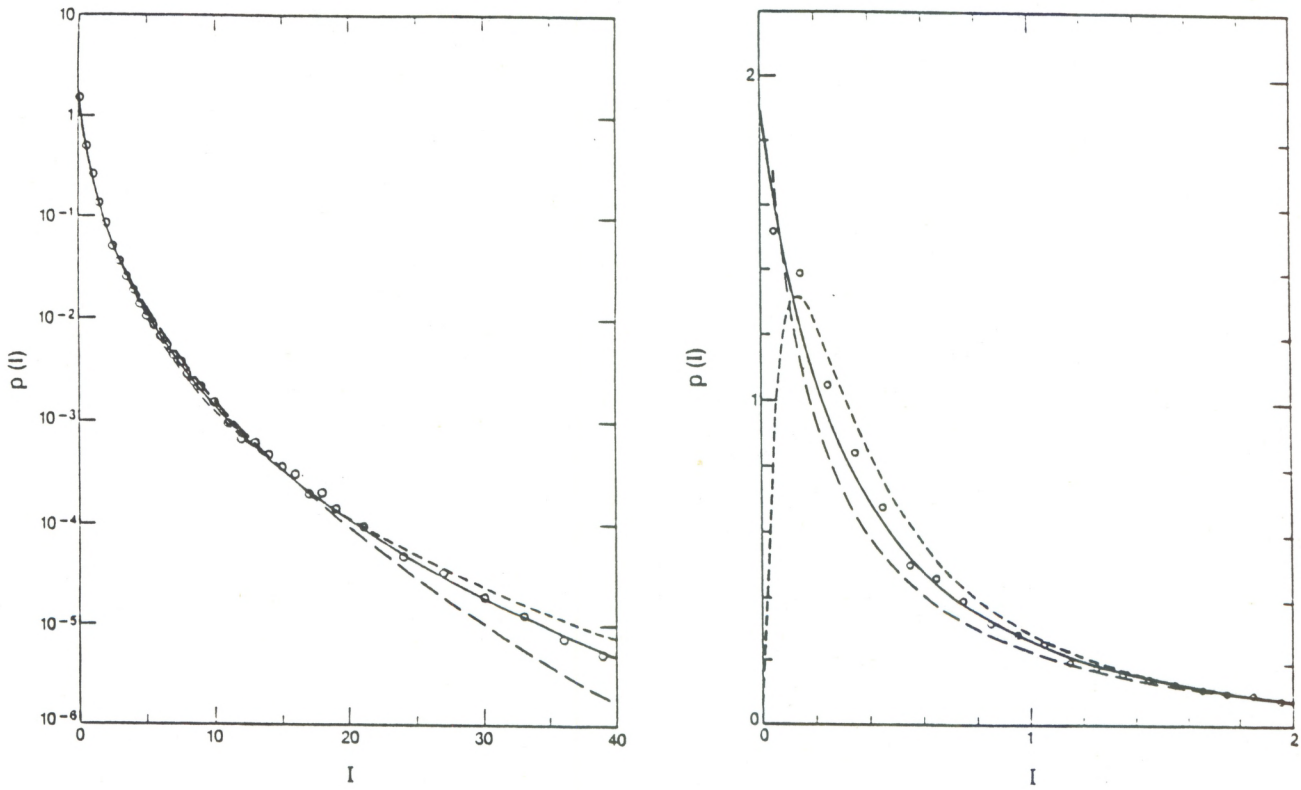

Figure 10. PDF of normalized irradiance for $\sigma_I^2 = 2.83$ ($\beta_o^2 = 36$): K (long-dashed curve), lognormal (short-dashed curve), lognormally modulated exponential (solid curve), and data (circles). (a) logarithmic representation; (b) linear representation for $I < 2$.

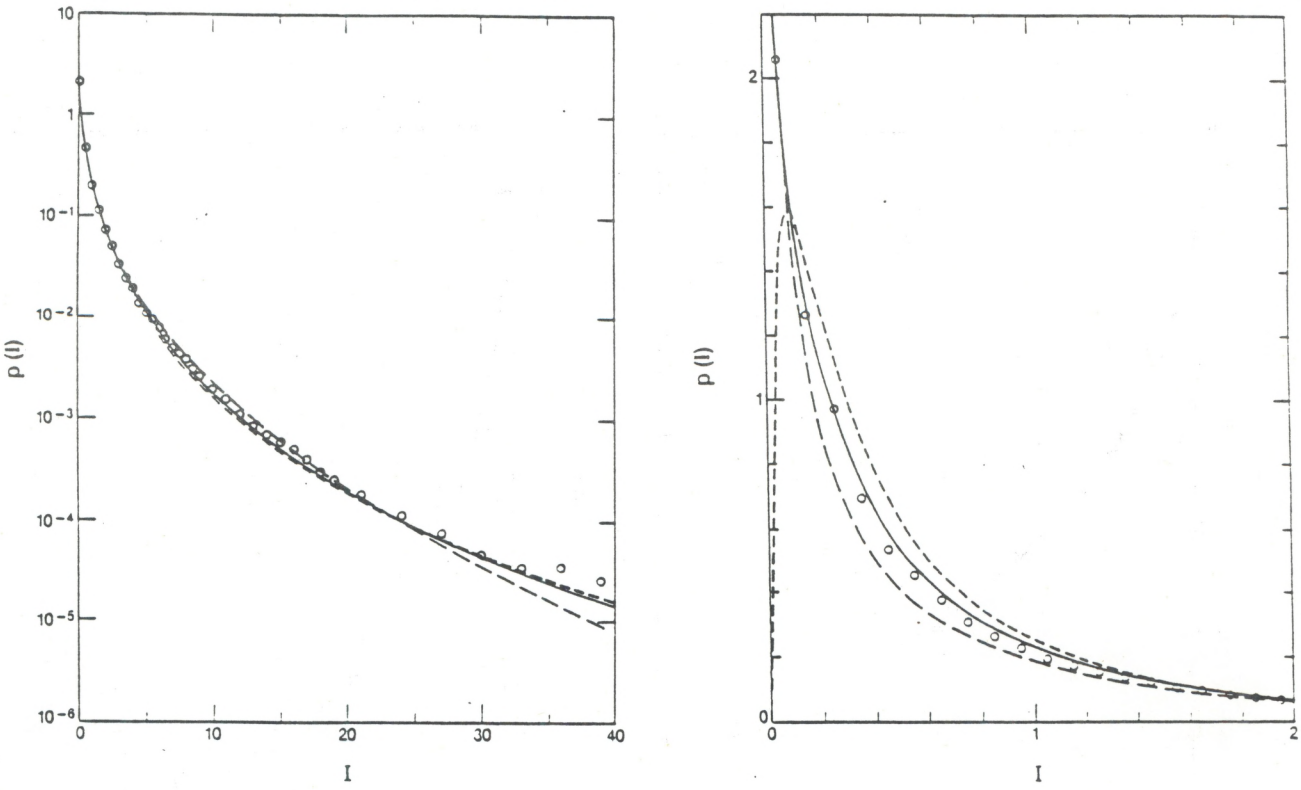

Figure 11. PDF of normalized irradiance for $\sigma_I^2 = 4.13$ ($\beta_o^2 = 23$): K (long-dashed curve), lognormal (short-dashed curve), lognormally modulated exponential (solid curve), and data (circles). (a) logarithmic representation; (b) linear representation for $I < 2$.

The propagation model that leads to the lognormally modulated exponential PDF suggests that the fluctuations due to the small-scale spikes of irradiance should be reduced by an aperture whose diameter is about a Fresnel zone size. The fluctuations observed through such an aperture would therefore be expected to be very nearly lognormally distributed. For this reason, a limited amount of data was taken through a 25–mm aperture. These data were, in fact, very nearly lognormal. Typical results are presented in Fig. 12. The solid line represents the lognormal probability density function with the same variance of irradiance ($\sigma_I^2 = 2.45$) as the data.

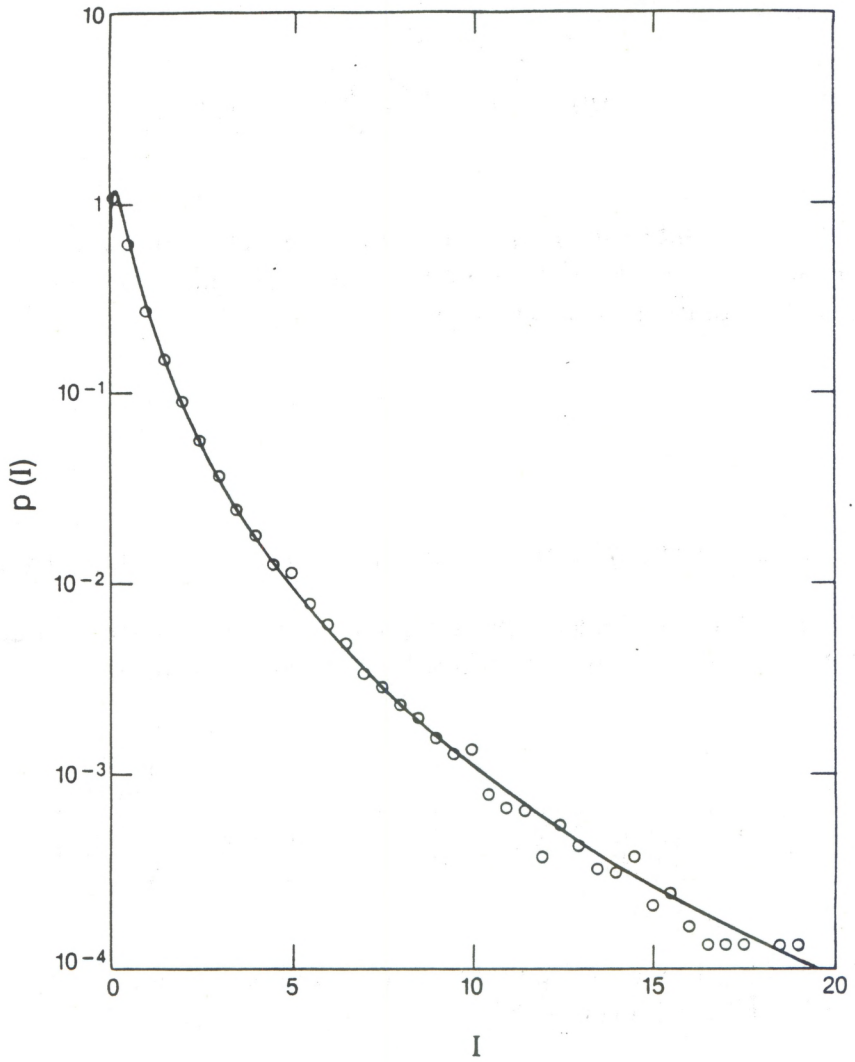

Figure 12. PDF of normalized irradiance through a 25–mm aperture: lognormal (solid curve) and data (circles), $\sigma_I^2 = 2.45$.

6.2 Photon-Count PDF

Since some of the previous work has dealt with the statistics of photon-counting experiments (Parry, 1981), it is interesting to examine the photon-count statistics produced by lognormally modulated exponential irradiance statistics. Photon counting allows the use of much smaller apertures than does use of irradiance measurements. If the spatial spikes of irradiance are progressively smaller in size for increasing irradiance (as suggested by Prokhorov et al., 1975) then we have underestimated our measured irradiance values because of aperture averaging by our 1–mm–diameter receiver aperture. Thus photon-count PDFs might be more trustworthy in the extreme tails of the PDF.

For counting times much less than the coherence time of the fluctuations, the probability density function of the photon count is a conditional Poisson process related to the irradiance PDF by the formula

$$p(n) = \int_0^\infty dI' \frac{(\gamma I')^n \exp(-\gamma I')}{n!} p(I') \ , \tag{56}$$

where γ is a constant related to the experimental configuration and I' is the actual (unnormalized) irradiance. For apertures much smaller than the transverse coherence length of the irradiance fluctuations, γ is given by

$$\gamma = \frac{AT}{h\nu} \ , \tag{57}$$

where A is the detector area, T is the count time, and $h\nu$ is photon energy.

Assuming that the irradiance obeys lognormally modulated exponential statistics, the photon-count statistics can be described by the density function

$$p(n) = \frac{1}{\sqrt{2\pi}\,\sigma_z \bar{n}} \int_0^\infty \frac{dz}{z^2} \left(1 + \frac{1}{\bar{n}z}\right)^{-n-1} \exp\left[-\frac{\left(\ell nz + \frac{1}{2}\sigma_z^2\right)^2}{2\sigma_z^2}\right] , \tag{58}$$

where $\bar{n}$ is the mean number of photon counts. The equivalent expression under the assumption of a K PDF is (Parry, 1981)

$$p(n) = \frac{\Gamma(M+n)}{\Gamma(M)} (M/\bar{n}) U(M+n,\ M,\ M/\bar{n}) \ , \tag{59}$$

where $M = 2/(\sigma_I^2 - 1)$ and $U(a,b,z)$ is a Kummer function (Parry, 1981).

In Figs. 13 and 14, we have reproduced, as circles, the photon count data obtained by Parry (1981). From his reported values of $\bar{n}$ and σ_I^2, we have calculated the corresponding curves for the K PDF, represented by long dashes, and the lognormally modulated exponential PDF, represented by a solid line. The short-dashed curve represents the K PDF photon-count statistics corrected for the effects of photomultiplier tube dead time, and was taken directly from Yura (1974). A similar correction, not shown, may be imagined for the lognormally modulated exponential PDF. The lognormally modulated exponential PDF is substantially closer to the data than is the K PDF.

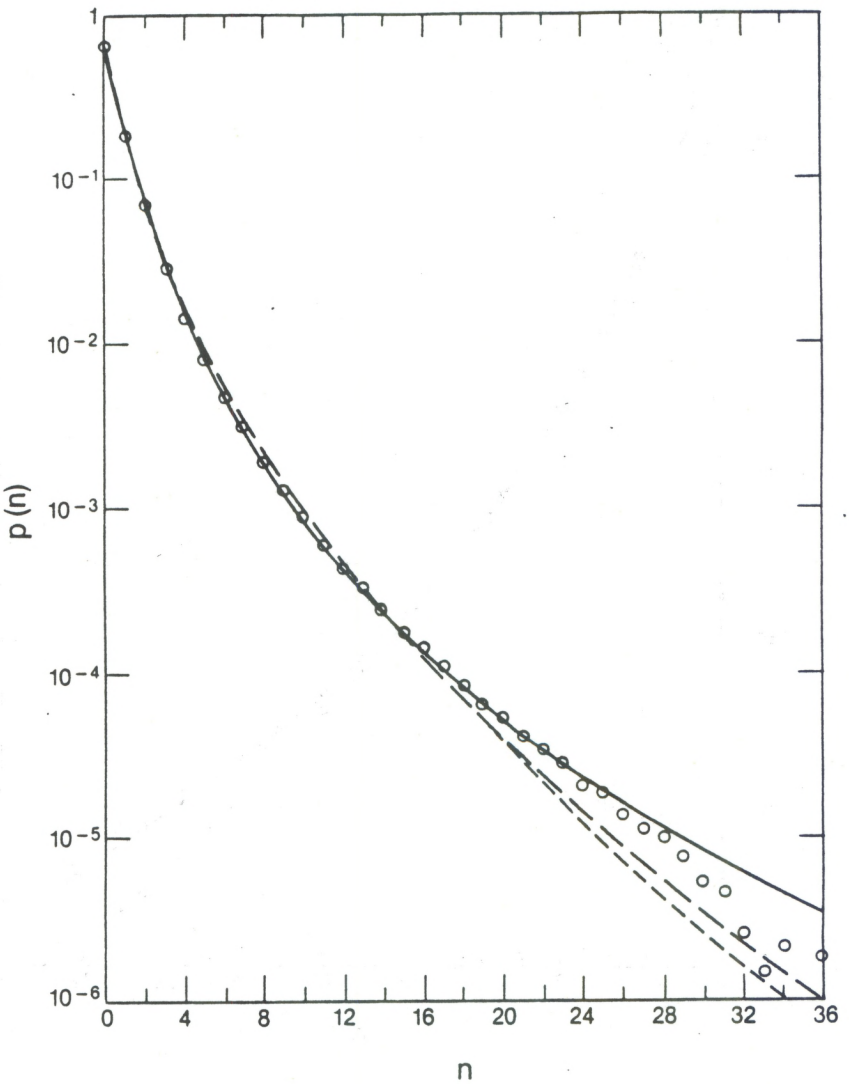

Figure 13. PDF of photon counts: K (long-dashed curve), dead-time corrected K (short-dashed curve), lognormally modulated exponential (solid curve), data from Fig. 7a of Parry and Pusey (1979) (circles).

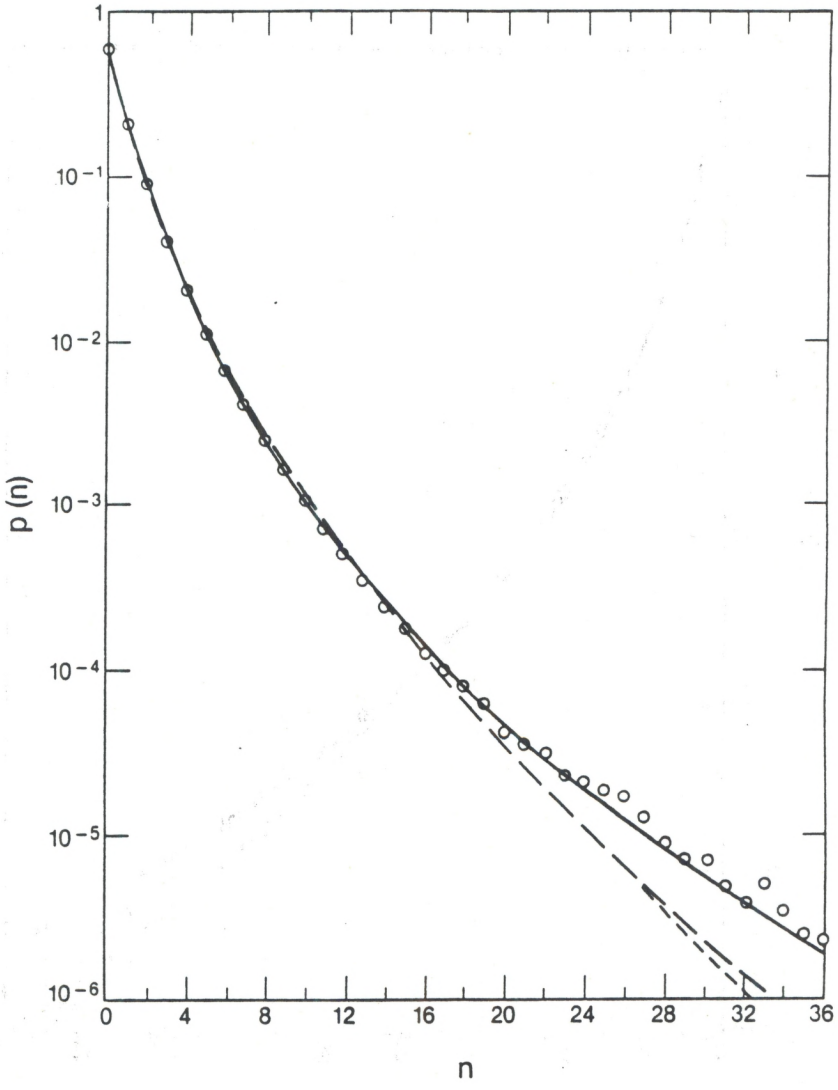

Figure 14. PDF of photon counts: K (long-dashed curve), dead-time corrected K (short-dashed curve), lognormally modulated exponential (solid curve), data from Fig. 7b of Parry and Pusey (1979) (circles).

6.3 Moments of Irradiance

Another method of comparing data with hypothesized probability density functions uses the moments of normalized irradiance

$$I_n = < I^n > \ . \tag{60}$$

Typically, third, fourth, and fifth moments are plotted as functions of the second moment or of the normalized variance, which is given by $I_2 - 1$. Discussions in the literature have considered moments up to eighth order (Majumdar, 1984).

For the lognormally modulated exponential PDF, evaluation of the nth moment is simple. Integration produces

$$I_n = n! \exp\left[\frac{1}{2} n(n-1)\sigma_z^2\right] . \tag{61}$$

We note that this expression is the first term in the asymptotic approach to exponential statistics obtained by Dashen (1984). The higher-order moments can be written in terms of the second moment as

$$I_n = n!(I_2/2)^{n(n-1)/2} , \tag{62}$$

provided that I_2 is greater than 2. If $I_2 = 2$, the variance of the lognormal modulation σ_z^2 is zero and the density function is the pure negative exponential that is expected in extreme saturation.

For the K PDF, the higher-order moments are given by

$$I_n = \frac{n!\Gamma\left(\frac{2}{I_2 - 2} + n\right)}{\left(\frac{2}{I_2 - 2}\right)^n \Gamma\left(\frac{2}{I_2 - 2}\right)} , \tag{63}$$

where Γ is the gamma function. Moments of the lognormal PDF are given by

$$I_n = I_2^{n(n-1)/2} . \tag{64}$$

The third, fourth, and fifth moments of these three distributions are plotted as functions of the second moment in Fig. 15. The moments of the lognormally modulated exponential lie between those of the other two density functions. For $I_2 = 2$, the lognormally modu-

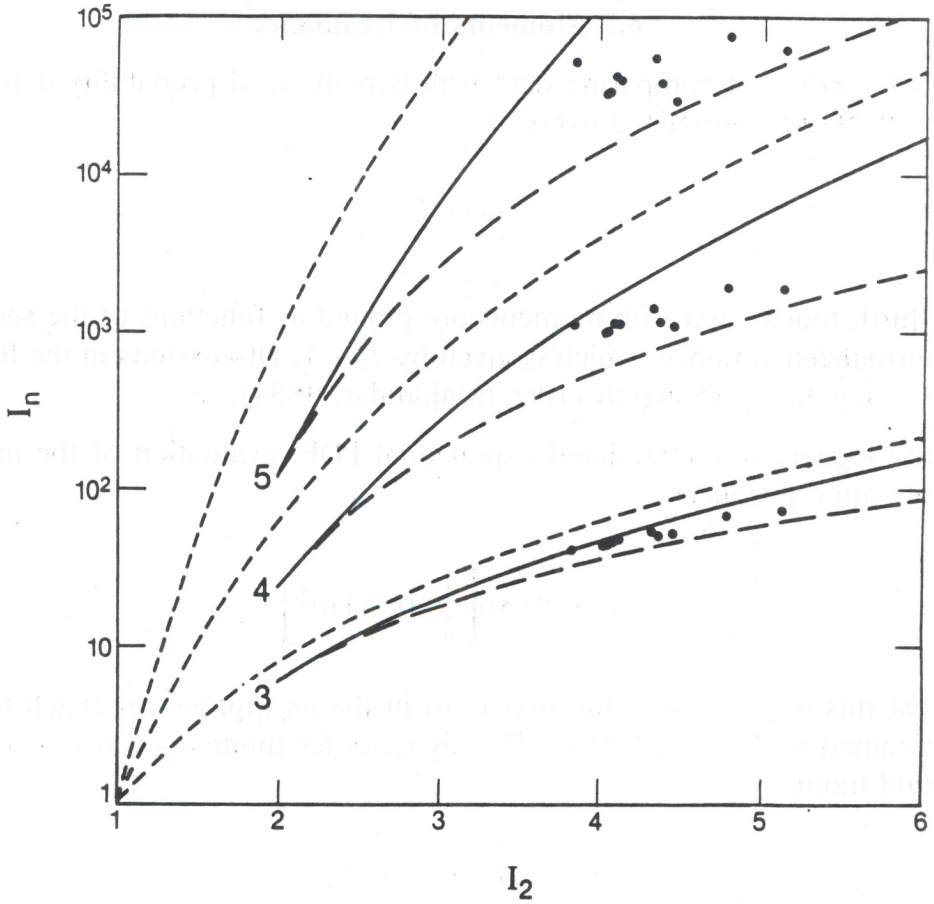

Figure 15. Third, fourth, and fifth normalized moments of irradiance, I_3, I_4, I_5 as functions of second moment I_2: K (long-dashed curves), lognormal (short-dashed curves), lognormally modulated exponential (solid curves), data (points).

lated exponential and the K density functions both reduce to the negative exponential PDF, and therefore have the same values of their moments. As the second moment increases, the higher-order moments of our function deviate from those of the K.

Experimentally measured moment values are also presented in Fig. 15. All the experimental values lie between those predicted by the K PDF and the log-normally modulated exponential PDF. Phillips and Andrews (1981) reported two data sets. In one, the data are consistently above the K values as observed here, but there is no obvious tendency for the higher moments to be closer to the K at the larger second-moment values. In their other data set, the higher moments do decrease relative to the K values as the second moment increases, and, in fact, they fall below the moments of the K PDF.

Despite the excellent agreement between experimental PDFs and the lognormally modulated exponential PDF in Figs. 10 and 11, the corresponding measured irradiance moments in Fig. 15 do not agree. The few samples having $I > 40$ and therefore not plotted

in Figs. 10 and 11 remain in agreement with the lognormally modulated exponential PDF. Extreme caution must be exercised in considering measured moments. Consortini and Conforti (1984), and Consortini et al. (1986) showed that the effects of detector saturation on the higher-order moments can be severe. In their work, the lognormal distribution and Furutsu distribution were considered.

The sensitivity of moments to large values of irradiance is easily seen from the integrand of the moment integral (Gracheva et al., 1978). The moments are given by

$$< I^n >= \int_0^\infty I^n p(I) dI \ . \tag{65}$$

The integrand, $I^n p(I)$, is plotted in Fig. 16 for several values of n. These curves assume a lognormally modulated exponential density function with a second moment of 4.5, which is typical of our data. Because the amplifier gain was optimized for each run of the experiment, our detector saturation voltage corresponds to values of I varying from about 40 to 100 depending on the run. All runs appear to be affected by saturation to some extent. Thus Fig. 16 shows that the fourth and fifth measured moments are greatly underestimated. Figure 16 also shows the need for extremely large sample spaces to reduce scatter in measured moments. To obtain accurate estimates of the third moment, Fig. 16 shows that several events near $I = 100$ should be observed. At $I = 100$, $p(I)$ is a little over 10^{-7} and several tens of millions of independent samples are needed. The required number of samples to resolve the fourth and fifth moments is much greater.

Because of these uncertainties in the measured moments we truncated the theoretical and experimental probability density functions at a value of $I = 40$ and recalculated the moments. The third, fourth, and fifth truncated moments are plotted as functions of the second truncated moment in Fig. 17. The higher moments of the data tend to lie just above those predicted by the lognormally modulated exponential PDF. They are well above those predicted by the K PDF and, in fact, are nearer to the lognormal than to the K. This resolves the contradiction between Fig. 16 and Figs. 10 and 11. Note that the scatter of the truncated measured moments in Fig. 17 is much less than the scatter of the untruncated measured moments in Fig. 15. We prefer truncating the PDFs to calculating the detector saturation effect because each of our runs has a different saturation intensity, thereby making graphical presentation difficult for the detector saturation calculation.

One statistic that should be less sensitive to truncation effects is the log-amplitude variance. This is because the integrand $(\ell nI - < \ell nI >)^2 p(I)$ is most sensitive to small values of I. For lognormal statistics we have the relationship

$$\sigma_\chi^2 = \frac{1}{4} \ell n I_2 \ , \tag{66}$$

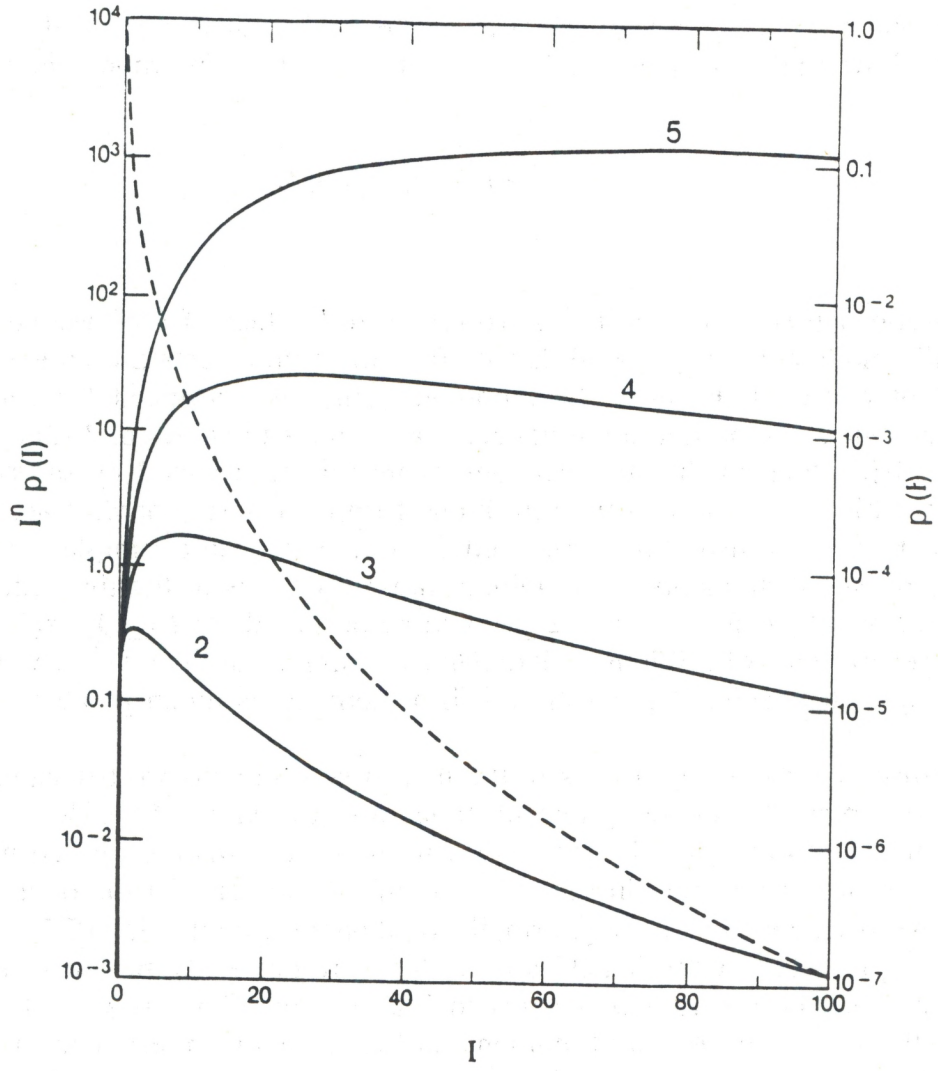

Figure 16. Second, third, fourth, and fifth moment integrands (solid curves) and irradiance PDF (dashed curve) for lognormally modulated exponential with $\sigma_l^2 = 3.5$.

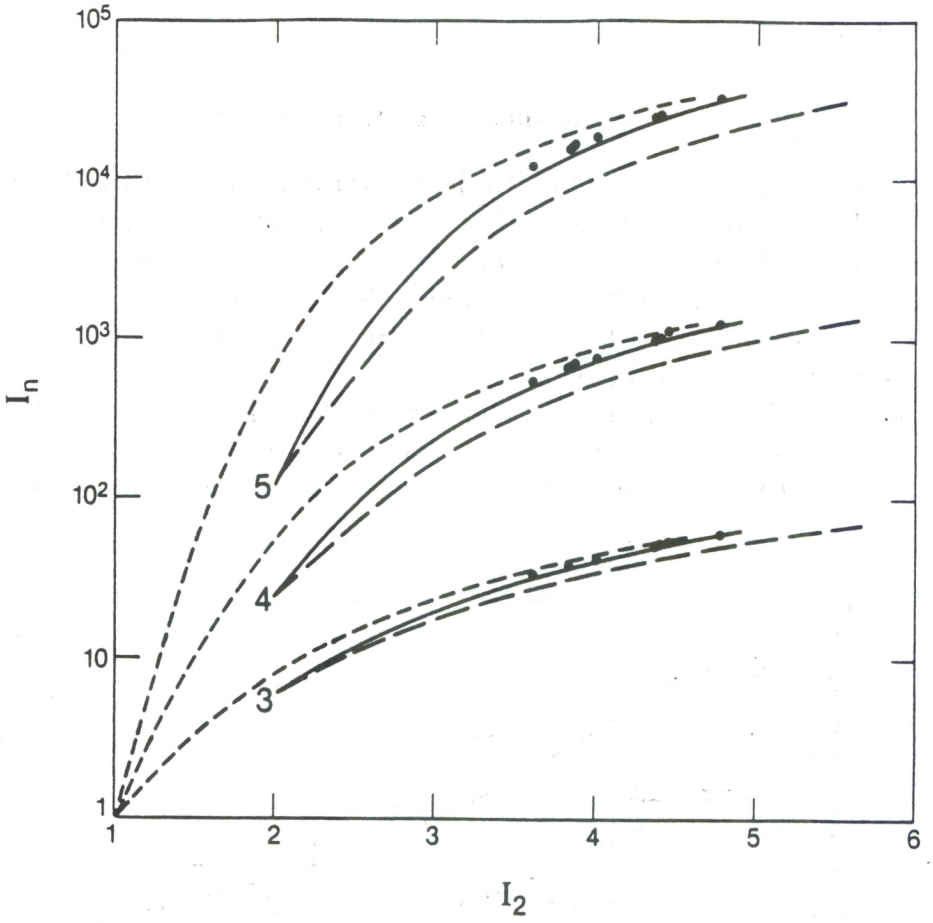

Figure 17. Third, fourth, and fifth normalized moments of irradiance, I_3, I_4, I_5 as functions of second moment I_2 for PDF truncated at I = 40 K (long-dashed curves), lognormal (short-dashed curves), lognormally modulated exponential (solid curves), data (points).

where σ_χ^2 is the log-amplitude variance. Clifford and Hill (1981) evaluated the log-amplitude variance of the K PDF to obtain

$$\sigma_\chi^2 = \frac{\pi^2}{24} + \frac{1}{4}\sum_{n=0}^{\infty}\left(n + \frac{2}{I_2 - 2}\right)^{-2} . \tag{67}$$

For the lognormally modulated exponential PDF the corresponding relationship is

$$\sigma_\chi^2 = \frac{\pi^2}{24} + \frac{1}{4}\ell n(I_2/2) . \tag{68}$$

As for the untruncated higher moments, the lognormally modulated exponential PDF predicts log-amplitude variance values that are between those of the lognormal and those of the K functions.

6.4 Variance of Irradiance

In order to determine how well the irradiance variance, and hence the parameter σ_z^2 could be inferred from the parameters of the medium, the normalized variance of irradiance was calculated for each data record, and the results from each group of 50 records were averaged and error bars calculated. Similarly, the average value of σ_R^2 and the error bars were found from the 50 samples of C_n^2. The result, a plot of measured intensity variance as a function of Rytov variance, is given in Fig. 18. The theoretical, zero-inner-scale curve is reproduced for comparison. Despite large error bars, the data can be seen to generally follow the shape of the theoretical curve. However, they lie consistently above it. This is probably due to non-zero inner scale. The inner scale under

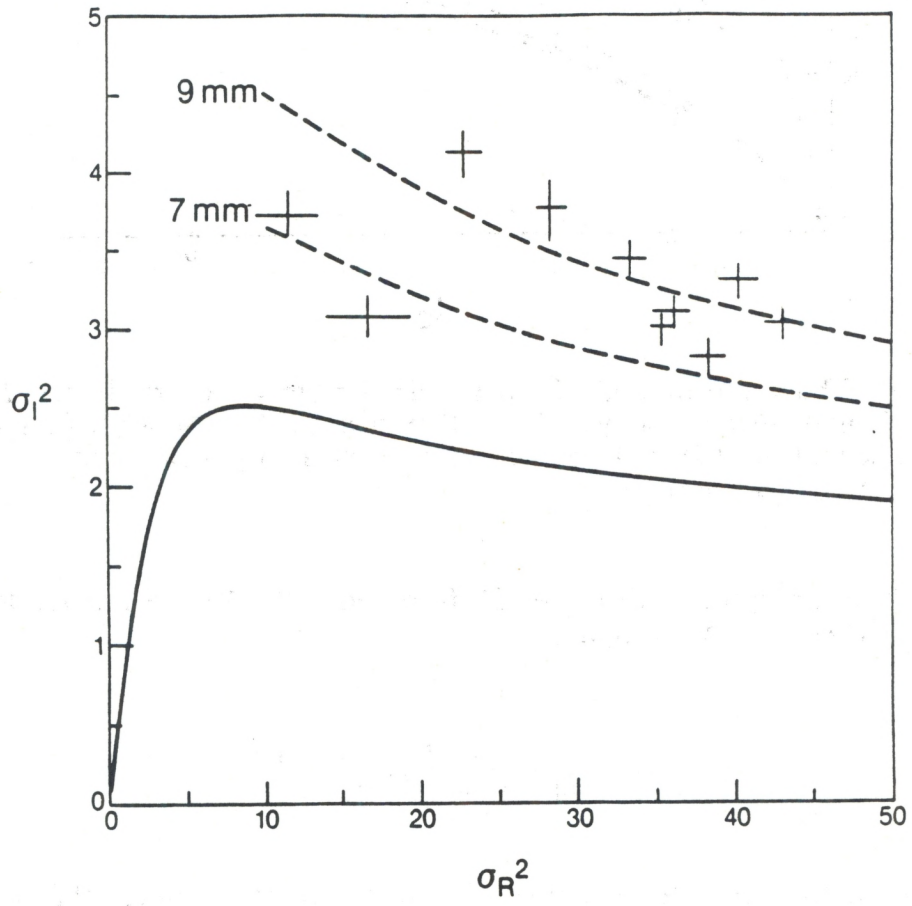

Figure 18. Normalized variance of irradiance σ_I^2 as a function of Rytov variance σ_R^2. The solid line represents zero-inner-scale theory, dashed lines include approximate inner scale correction for 7-mm and 9-mm inner scales, and points represent measured values, including error bars.

the conditions for which these data were taken is generally between about 7 mm and about 9 mm. Hill and Clifford (1981) showed that the increase in log-amplitude variance due to an inner scale of 7 mm is about 50% for σ_R^2 greater than about 10. For a 9–mm inner scale, the corresponding increase is about 80%. If we assume that the effect of inner scale on σ_z^2 is the same as the effect on log-amplitude variance calculated in Hill and Clifford (1981) and Hill (1982), we obtain the dashed lines in the figure. Clearly, much better agreement with the data is seen when the effects of inner scale are approximated. Note also that the peak irradiance values for 7–mm to 9–mm inner scales are in the range reported in other experiments (Parry and Pusey, 1979; Parry, 1981; Phillips and Andrews, 1981).

As Fig. 18 suggests, the results in this regime are extremely sensitive to the precise value of the inner scale. For example, the change in normalized variance $\Delta\sigma_I^2$ due to a change in inner scale size $\Delta\ell_o$ was estimated for the experimental geometry with σ_R^2 of 30 and an inner scale of 7 mm. We assumed that the variance could be represented by

$$\sigma_I^2 = 2\exp(a\sigma_z^2) - 1 \ , \tag{69}$$

where a includes the effects of inner scale and σ_z^2 is the zero-inner-scale value. From Table 1 of Hill (1982) a can be found from

$$a(\sqrt{\lambda L}\,/\ell_o) = \sigma_\chi^2(\sqrt{\lambda L}\,/\ell_o)/\sigma_\chi^2(\infty) \ . \tag{70}$$

It turns our that the logarithm of this quantity is very nearly linear in $\sqrt{\lambda L}\,/\ell_o$; a linear regression for the case of $\sigma_R^2 = 32$ results in

$$\ell n\ a = 1.2 - 0.22\sqrt{\lambda L}\,/\ell_o \ . \tag{71}$$

The derivative of variance with respect to inner scale can then be taken. At 7 mm, the result is

$$\Delta\sigma_I^2 \approx 0.3 mm^{-1}\Delta\ell_o \tag{72}$$

for small changes in inner scale.

7. REFLECTED BEAMS

The probability density function of a reflected beam can be found by treating the reflector as a secondary source. The power transmitted by this source is proportional to

the power incident on the reflector and is a random variable because of turbulence effects on the outgoing path. The conditional signal at the receiver for a given reflected power is also a random variable due to turbulence effects on the return path. The total PDF is given by

$$p(P_s) \int p(P_s|P_r)p(P_r)dP_r \,, \tag{73}$$

where $p(P_s|P_r)$ is the conditional PDF of received signal power P_s given the reflected power P_r, and $p(P_r)$ is the PDF of the reflected power.

If the reflector is small (diameter < ϱ_o), the reflected power will have a lognormally modulated Rician PDF. A larger aperture would produce a lognormal PDF. The latter is probably the more common case. Note that if the target intercepts the entire beam, the reflected power will be constant and $p(P_r)$ is a delta function.

The conditional PDF of the reflected beam depends on the characteristics of the target and of the receiver. For a small specular or retroreflecting target, the target can be treated as a point source. Therefore, a small receiver will see a LR conditional PDF. In this case, both the conditional PDF $p(P_s|P_r)$ and the PDF $p(P_r)$ are lognormally modulated Rician, and the full PDF, which can be obtained from Eq. (73), is very complicated.

For a small target and a larger receiver aperture, the conditional PDF will be lognormal. In this case, the received power is given by the reflected power times a lognormal modulation factor caused by turbulence on the return path. The reflected power is given by the product of a Rician random variable and another lognormal modulation factor. Therefore, the received power is the product of a Rician random variable and two lognormal random variables. Since the product of two lognormal random variables is lognormal (Papoulis, 1965), the received power will have a LR PDF. Note that a large target and a small receiver aperture will also produce a LR PDF for the same reason.

If the aperture and the target are both large, the conditional PDF and the PDF of reflected power will both be lognormal. Therefore, the received power will also be lognormal.

For diffuse targets, an extra modulation factor in the received power must be considered. This "speckle" factor has a negative exponential PDF, and the conditional PDF must also be integrated over this PDF. However, if the receiver is larger than the speckle size, this factor can be neglected and the previous results hold. This is an easy condition to satisfy since the speckle size is given by (Goodman, 1968)

$$D_s = 2.44\lambda D_r/L \tag{74}$$

where λ is the optical wavelength, D_r is the reflector diameter, and L is the path length.

8. CONCLUSIONS

We conclude that the lognormally modulated Rician (LR) probability density function (PDF) more nearly represents optical propagation through turbulence than does the IK PDF. For systems using apertures larger than the phase coherence length ϱ_o, the lognormal PDF seems to be a reasonable model.

Acknowledgments

This research was partially supported by the U.S. Army Atmospheric Sciences Laboratory under military interdepartmental purchase request ASL 87-8013.

9. REFERENCES

Andrews, L.C., and R.L. Phillips (1985): I-K distribution as a universal propagation model of laser beams in atmospheric turbulence. *J. Opt. Soc. Am. A*, **2**, 160–163.

Barakat, R. (1976): Sums of independent lognormally distributed random variables. *J. Opt. Soc. Am.*, **66**, 211–216.

Bissonnette, L.R., and P.L. Wizinowich (1979): Probability distribution of turbulent irradiance in a saturation regime. *Appl. Opt.*, **18**, 1590–1599.

Bissonnette, L.R. (1983): Propagation model of laser beams in turbulence. *J. Opt. Soc. Am.*, **73**, 262–268.

Clifford, S.F., and R.J. Hill (1981): Relation between irradiance and log-amplitude variance for optical scintillation described by the K distribution. *J. Opt. Soc. Am.*, **71**, 112–114.

Clifford, S.F., G.R. Ochs, and R.S. Lawrence (1974): Saturation of optical scintillation by strong turbulence. *J. Opt. Soc. Am.*, **64**, 148–154.

Coles, W.A., and R.G. Frehlich (1982): Simultaneous measurements of angular scattering and intensity scintillation in the atmosphere. *J. Opt. Soc. Am.*, **72**, 1042–1048.

Consortini, A., and G. Conforti (1984): Detector saturation effect on higher-order moments of intensity fluctuations in atmospheric laser propagation measurement. *J. Opt. Soc. Am. A*, **1**, 1075–1077.

Consortini, A., and L. Ronchi (1977): Probability distribution of the sum of N complex random variables. *J. Opt. Soc. Am.*, **67**, 181–185.

Consortini, A., E. Briccolani, and G. Conforti (1986): Strong-scintillation-statistics deterioration due to detector saturation. *J. Opt. Soc. Am. A*, **3**, 101–107.

Dashen, R. (1979): Path integrals for waves in random media. *J. Math. Phys.*, **20**, 894–922.

Dashen, R. (1984): Distribution of intensity in a multiply scattering medium. *Opt. Lett.*, **9**, 110–112.

Deitz, P.H., and N.J. Wright (1969): Saturation of scintillation magnitude in near-earth optical propagation. *J. Opt. Soc. Am.*, **59**, 527–535.

DeWolf, D.A. (1968): Saturation of irradiance fluctuations due to turbulent atmosphere. *J. Opt. Soc. Am.*, **58**, 461–466.

DeWolf, D.A. (1969): Are strong irradiance fluctuations lognormal or Rayleigh distributed? *J. Opt. Soc. Am.*, **59**, 1455–1460.

DeWolf, D.A. (1974): Waves in turbulent air: a phenomenological approach. *Proc. IEEE*, **62**, 1523–1529.

Fante, R.L. (1983): Inner-scale size effect on the scintillations of light in the turbulent atmosphere. *J. Opt. Soc. Am.*, **73**, 277–281.

Fremouw, E.J., R.C. Livingston, and D.A. Miller (1980): On the statistics of scintillating signals. *J. Atmos. Terr. Phys.*, **42**, 717–731.

Fried, D.L., G.E. Mevers, and M.P. Keister, Jr. (1967): Measurements of laser-beam scintillation in the atmosphere. *J. Opt. Soc. Am.*, **57**, 787–797.

Furutsu, K. (1972): Statistical theory of wave propagation in a random medium and the irradiance distribution function. *J. Opt. Soc. Am.*, **62**, 240–254.

Furutsu, K. (1976): Theory of irradiance distribution function in turbulent media—cluster approximation. *J. Math. Phys.*, **17**, 1252–1263.

Furutsu, K. (1979): Review of the theory of the irradiance distribution function in a turbulent media with a particular emphasis on analytical methods. *Radio Sci.*, **14**, 287–299.

Gochelashvili, K., and V.S. Shishov (1971): Laser beam scintillation beyond a turbulent layer. *Opt. Acta*, **18**, 313–320.

Goodman, J.W. (1968): *Fourier Optics*, McGraw-Hill, New York, 65.

Gracheva, M.E. (1967): Investigation of the statistical properties of strong fluctuations in the intensity of light propagated through the atmosphere near the earth. *Izv. VUZ. Radiofiz.*, **10**, 775–778.

Gracheva, M.E., and A.S. Gurvich (1965): Strong fluctuations in the intensity of light propagated through the atmosphere close to the earth. *Izv. VUZ. Radiofiz.*, **8**, 717–724.

Gracheva, M.E., A.S. Gurvich, S.S. Kashkarov, and Vi.V. Pokasov (1978): Similarity relations and their experimental verification for strong intensity fluctuation of laser radiation. In *Laser Beam Propagation in the Atmosphere*, J.W. Strohbehn, ed. (Springer-Verlag, New York) 107–127.

Gurvich, A.S., M.A. Kallistratova, and N.S. Time (1968): Fluctuations in the parameters of a light wave from a laser during propagation in the atmosphere. *Izv. VUZ. Radiofiz.*, **11**, 1360–1370.

Hill, R.J. (1982): Theory of saturation by strong turbulence: plane-wave variance and covariance and spherical-wave covariance. *J. Opt. Soc. Am.*, **72**, 212–222.

Hill, R.J., and S.F. Clifford (1978): Modified spectrum of atmospheric temperature fluctuations and its application to optical propagation. *J. Opt. Soc. Am.*, **68**, 892–899.

Hill, R.J., and S.F. Clifford (1981): Theory of saturation of optical scintillation by strong turbulence for arbitrary refractive-index spectra. *J. Opt. Soc. Am.*, **71**, 675–686.

Ito, S., and K. Furutsu (1982): Theoretical analysis of the high-order irradiance moments of light waves observed in turbulent air. *J. Opt. Soc. Am.*, **72**, 760–764.

Jakeman, E., and P.N. Pusey (1976): A model for non-Rayleigh sea echo. *IEEE Trans. Antennas Propagat.*, **AP-24**, 806–814.

Jakeman, E., and P.N. Pusey. (1978): Significance of K distributions in scattering experiments. *Phys. Rev. Lett.*, **40**, 546–550.

Knepp, D.L., and G.C. Valley (1978): Properties of joint Gaussian statistics. *Radio Sci.*, **13**, 59–68.

Majumdar, A.K. (1984): Higher-order statistics of laser-irradiance fluctuations due to turbulence. *J. Opt. Soc. Am. A*, **1**, 1067–1074.

Mitchell, R.L. (1968): Permanence of the log-normal distribution. *J. Opt. Soc. Am.*, **58**, 1267–1272.

Newman, D. (1985): K distributions from doubly scattered light. *J. Opt. Soc. Am. A*, **2**, 22–26.

Ochs, G.R., and R.S. Lawrence (1969): Saturation of laser-beam scintillation under conditions of strong atmospheric turbulence. *J. Opt. Soc. Am.*, **59**, 226–227.

Papoulis, A. (1965): *Probability, Random Variables, and Stochastic Processes*. McGraw-Hill, New York, 205.

Parry, G. (1981): Measurement of atmospheric turbulence induced intensity fluctuations in a laser beam. *Opt. Acta*, **28**, 715–728.

Parry, G., and P.N. Pusey (1979): K distributions in atmospheric propagation of laser light. *J. Opt. Soc. Am.*, **69**, 796–798.

Parry, G., P.N. Pusey, E. Jakeman, and J.G. McWhirter (1977): Focusing by a random phase screen. *Opt. Commun.*, **22**, 195–201.

Phillips, R.L., and L.C. Andrews (1981): Measured statistics of laser-light scattering in atmospheric turbulence. *J. Opt. Soc. Am.*, **71**, 1440–1445.

Phillips, R.L., and L.C. Andrews (1982): Universal statistical model for irradiance fluctuations in a turbulent medium. *J. Opt. Soc. Am.*, **72**, 864–870.

Prokhorov, A.M., F.V. Bankin, K.S. Goschelashvily, and V.I. Shishov (1975): Laser irradiance propagation in turbulent media. *IEEE Proc.*, **63**, 790–811.

Rino, C.L., R.C. Livingston, and H.E. Whitney (1976): Some new results on the statistics of radio wave scintillation. I. Empirical evidence for Gaussian statistics. *J. Geophys. Res.*, **81**, 2051–2057.

Strohbehn, J.W. (1978): Modern theories in the propagation of optical waves in a turbulent medium. In *Laser Beam Propagation in the Atmosphere*, J.W. Strohbehn, ed. (Springer-Verlag, New York) 45–106.

Strohbehn, J.W., T. Wang, and J.P. Speck (1975): On the probability distribution of line-of-sight fluctuations of optical signals. *Radio Sci.*, **10**, 49–70.

Tatarskii, V.I. (1971): *The Effects of a Turbulent Atmosphere on Wave Propagation*. (Israel Program for Sci. Trans., Jerusalem, 1971).

Valley, G.C., and D.L. Knepp (1976): Application of joint Gaussian statistics to interplanetary scintillation. *J. Geophys. Res.*, **81**, 4723–4730.

Wang, Ting-i, and J.W. Strohbehn (1974): Log-normal paradox in atmospheric scintillations. *J. Opt. Soc. Am.*, **64**, 583–591.

Wang, Ting-i, and J.W. Strohbehn (1974): Perturbed log-normal distribution of irradiance fluctuations. *J. Opt. Soc. Am.*, **64**, 994–999.

Yura, H.T. (1974): Physical model for strong optical-amplitude fluctuation in a turbulent medium. *J. Opt. Soc. Am.*, **64**, 59–67.